The Strength of Metals under Combined Alternating Bending and Torsion.

By

Toshio Nishihara and Minoru Kawamoto.

Abstract.

Fatigue tests under combined bending and torsion were carried out for several ferreous and nonferreous metals with a testing machine specially designed. As the results of tests, strength of metals under combined alternating bending and torsion were expressed by a simple relation, using fatigue strength of each metals under simple bending and torsion. And some considerations about fatigue fracture were made.

I. Introduction.

The studies on the strength of materials under repeated stresses have been executed mostly under simple stress conditions; such as direct, bending, or torsional stresses. But the majority of engineering problems of fatigue are concerned with combined stress distribution. Among several combinations of these simple stresses, the case of combined cyclic bending and torsion is most usually encountered in the practical design. Under this condition of the combined stresses, however, few experiments have been made hitherto. Stanton[1] and Batson devised a modified form of the rotating bar fatigue testing machine. Their idea is somewhat interesting but the machine is hardly available in practice because of the unavoidable vibration. Gough[2] and Pollard used a fatigue testing machine of the cantilever type and made experiments for two ductile steels and a silcon cast iron.

The authors have recently devised a new combined stress testing machine and carried out the experiments on the fatigue strength of metalic materials under combined bending and torsion. The machine utilizes the inertia force of the oscillating fly wheel and the specimen is subjected to uniform bending and torsional moments. While the present paper reports the test results in the case of combinations of alternating bending and torsional stresses, it is also capable, by adding simple attachments to the machine, to make the experiments when the mean stresses are existing. This fact makes this machine easily available when the mean stress is commonly not zero, as in the case of general engineering problems.

The test materials used in the present investigation are the following nine kinds of metalic materials; that is, mild, medium and high carbon steels, an alloy steel, a cast iron, a brass, and two kinds of aluminium light alloys. The fatigue limits were determined by endurance tests, using the combined fatigue testing machine above described. In conducting the tests, seven different ratio of combinations of bending and torsional stresses were adopted for some materials. But for other materials, five combinations or even only three combinations were adopted, when regarded as sufficient to determine the criterion of fatigue failure of the materials.

II. Description of a New Combined Bending and Torsional Fatigue Testing Machine.

Fig. 1 is the explanative skeleton of the principle of the machine. One end of the specimen S is clamped to the main shaft A to which the fly wheel F is attached. The other end is clamped to the supplementary shaft B, vibrated by a crank and eccentric mechanism with any desired amplitude. The specimen may be clamped at any position to the shaft B; so that the longitudinal

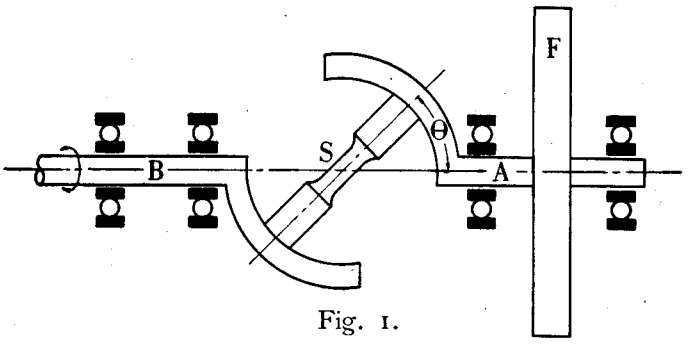

Fig. 1.

axis of the specimen makes an angle θ with the axis of the shaft A or B. As the vibration of the shaft B is transmitted through the specimen to the fly wheel, cycles of reversed bending and torsional moment are imposed on the specimen by inertia forces of the fly wheel and the shaft A. Then

(1) Stanton, T. E., Batson, R. G., Engineering, 1916, vol. CII, p. 269.
(2) Gough, H. J., and Pollard, H. V., Proc. I. Mech. E., 1935, vol. 131, p. 3.

the bending moment applied to the specimen is proportional to $\sin\theta$ and the torque proportional to $\cos\theta$. It will be noted that the bending moment and torque are reversed in the same phases, so that they reach their maximum and minimum values simultaneously. When θ makes 0 deg., cycles of reversed torsion are applied, and when θ is 90 deg., cycles of reversed uniform bending are applied, while any desired combination of bending and torsion is available by an appropriate choise of the value of θ.

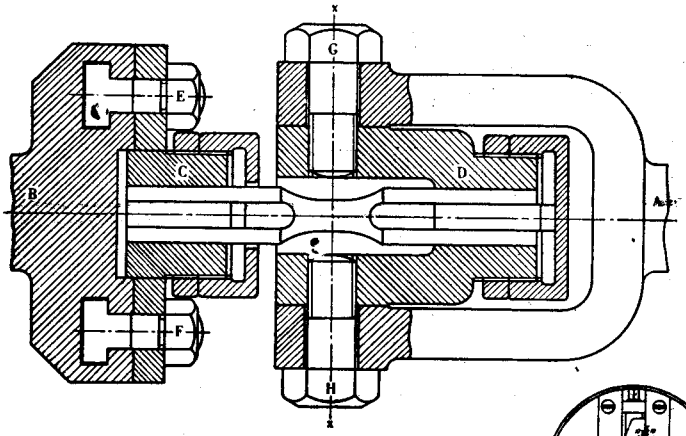

Fig. 2.

Fig. 2 shows the method of clamping the specimen to the shafts A and B. Both ends of the specimen are keyed to chucks C and D, respectively. The chuck C can be rotated about the center line XX as an axis, and clamped with two bolts E and F to any position on the end surface of the shaft B which has the shape of a quadrant. The chuck D is then clamped with two bolts G and H in the forked end of the shaft A.

The general arrangement of the machine is shown in Fig. 3. The machine is driven by a belt at constant speed. The amplitude of the vibration of the fly wheel is precisely adjustable by changing the effective length of the crank arm without stopping the machine and can be measured precisely with the accuracy of about 0.01 deg. by an optical slit devise. It must be noted that this machine should not be operated at a speed over the resonant or critical. The resonant speed varies according to the material and the diameter of the specimen and also the angle θ. The resonant speed becomes higher as θ increases ordinarily. In the experiments described here the speed of the machine was kept, in most cases, at 1700 stress cycles per minute, though the resonant speed was sometimes much higher. Only in cases of duralumins the tests were carried out at the speed of 1400 stress cycles per minute owing to the low resonant speed.

To determine the value of the moment applied to a specimen, the moment of inertia of the fly wheel and the shaft A must be known.

Let

I=The moment of inertia, kg·cm·sec^2
a=Amplitude of the fly wheel, radian
n=The number of stress repetitions per minute
M=Maximum moment applied to a specimen

Then

$$M=Ia\left(\frac{\pi n}{30}\right)^2$$

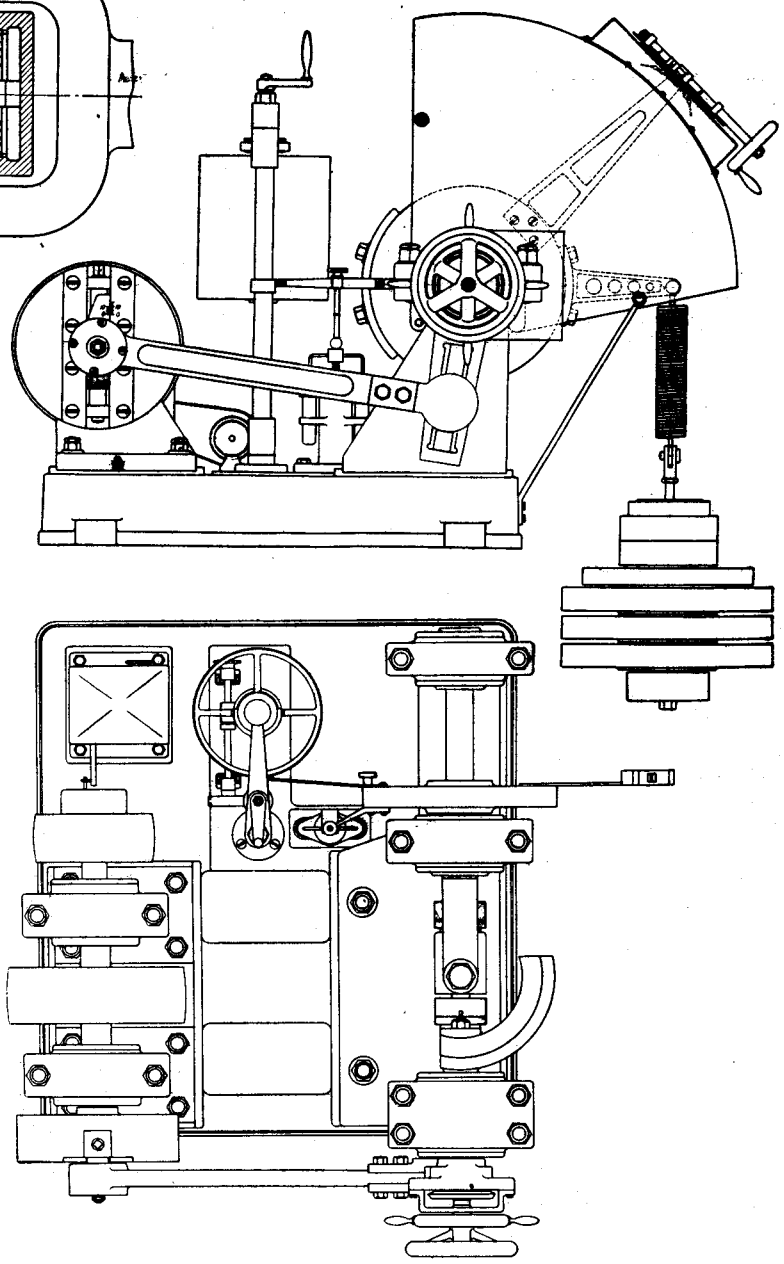

Fig. 3.

General Arrangement of the Combined Bending and Torsional Fatigue Testing Machine.

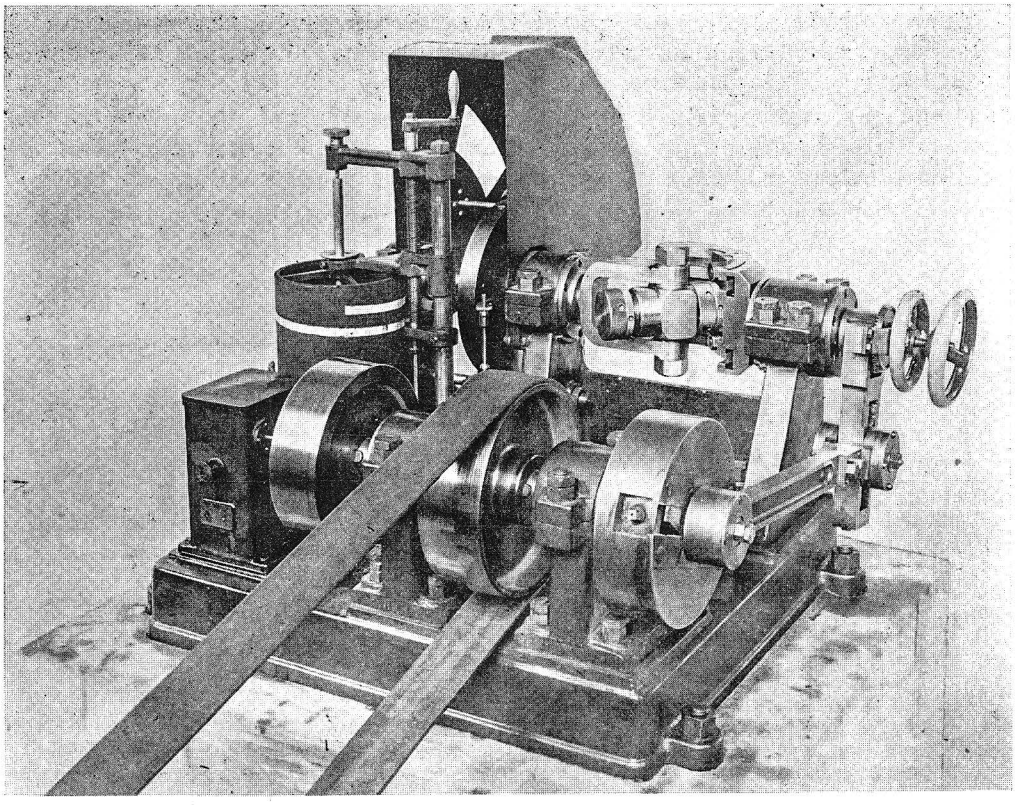

Fig. 4. The Combined Bending and Torsional Fatigue Testing Machine.

The value of I is found by calculation, measuring the dimension of each part and it was as follows.

When $\theta = 0$ deg., $I = 0.753$ kg·cm·sec^2
30 ,, 0.765 ,,
60 ,, 0.789 ,,
90 ,, 0.801 ,,

Fig. 4 is the photograph of the testing machine adjusted as θ to be 45 degree.

III. Material Used and Forms of Specimens Employed.

The following nine materials were used.

(1) Mild steel received in the form of bar 28 mm in diameter and 5 m in length.
(2) Medium steel received in the form of bar 32 mm in diameter and 5 m in length.
(3) Swedish high carbon steel received in the form of bar 25 mm in diameter and 2 m in length.
(4) Nickel-chromium steel received as hot-rolled in the form of bar 25 mm in diameter and 4 m in length.
(5) The same nickel-chromium steel heat-treated in the laboratory.
(6) Gray cast iron bars made in the laboratory.
(7) Duralumin extruded in the form of bar 26 mm in diameter and 2 m in length.
(8) Duralumin extruded in the form of bar 24 mm in diameter and 2 m in length.
(9) Brass extruded in the form of bar 30 mm in diameter and 3 m in length.

Both ends of each bar, about 10 cm in length, were excluded from the tests. Before tests were made, mild steel, medium steel and high carbon steel were heat-treated as shown in Table 2, at the

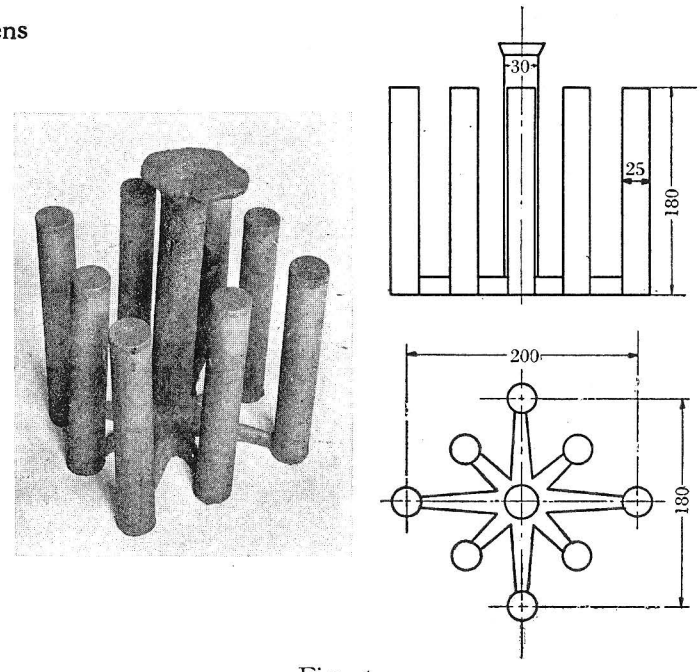

Fig. 5.

laboratory. Special attention was given to the moulding shape of cast iron, because it influences the properties of cast iron. As shown in Fig. 5, eight rods of 25 mm in diameter and 180 mm in length were made as one casting.

A chemical analysis and microscopical examination was carried out on samples of each material investigated. The results of the chemical analysis are shown in Table 1, and those of microscopical examination in Fig. 6.

The forms and dimensions of the specimens employed are given in Fig. 7. The fatigue specimens have, in each case, some parallel parts and the fillet radii of twice the diameters of the parallel

Table 1.

Chemical Composition of Materials.

Materials	Chemical Composition in %												
	C	Mn	S	P	Si	Ni	Cr	Fe	Al	Mg	Cu	Zn	Pb
Mild Steel	0.07	0.30	0.040	0.040	0.14								
Medium Steel	0.34	0.48	0.028	0.016	0.24								
Hard Steel	0.62	0.23	0.010	0.024	0.27								
Nickel-Chromium Steel	0.42	0.52	0.02	0.016	0.27	1.76	0.66				0.21		
Cast Iron	Total 3.15 Graphitic 2.34	0.39	0.12	0.44	1.95						0.10		
Duralumin D-26		0.46			0.33			0.41		0.41	3.60		
Duralumin D-24		0.44			0.38			0.43		0.47	3.71		
Brass								0.02			70.08	29.88	0.01

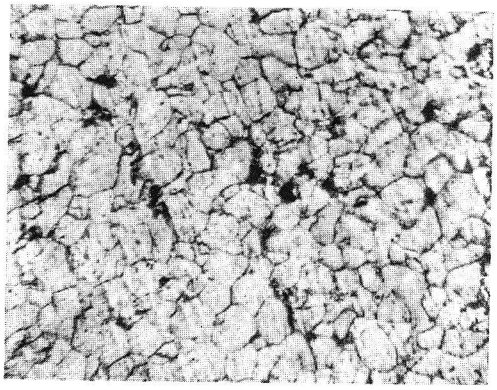

Mild Steel (Cross Section) ×175

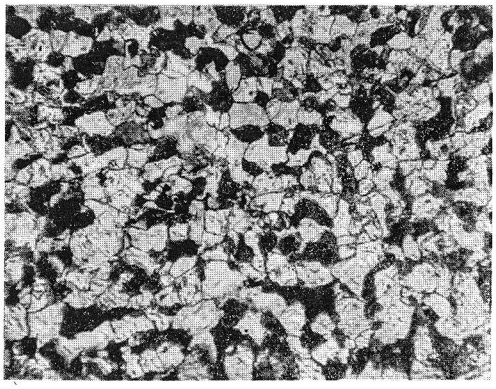

Medium Steel (Cross Section) ×175

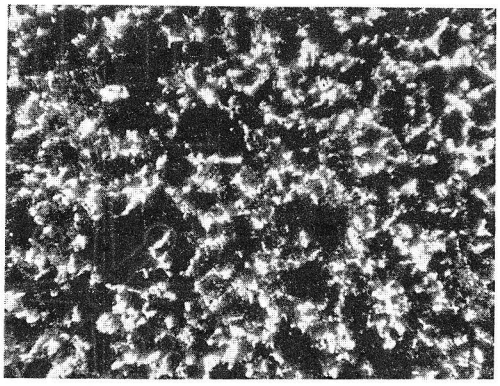

Hard Steel (Cross Section) ×175

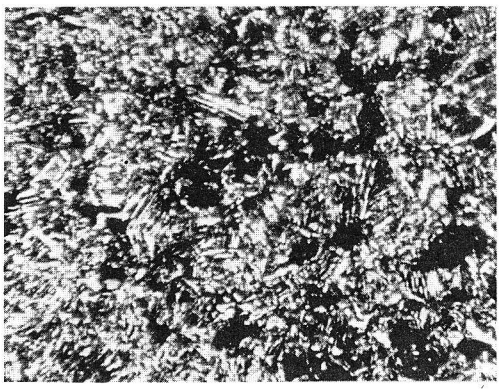

Nickel-Chromium Steel, Hot-rolled (Cross Section) ×175

Fig. 6 (a). Microscopical Structures of Materials.

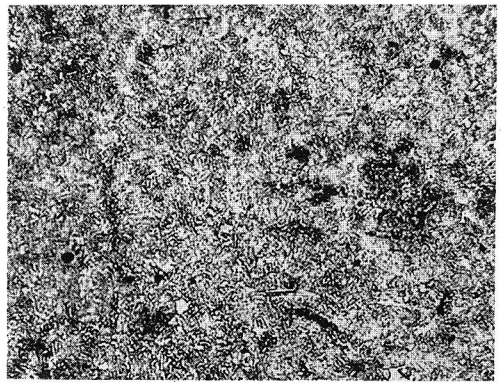

Nickel-Chromium Steel, Heat-treated (Cross Section) ×175

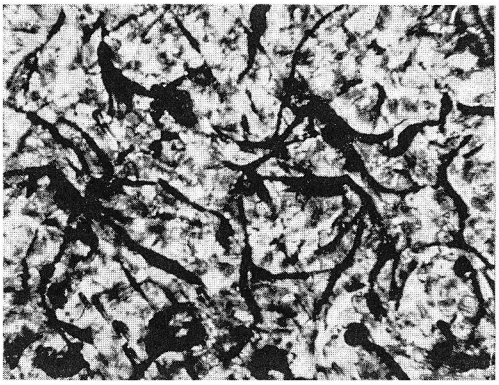

Cast Iron (Cross Section) ×175

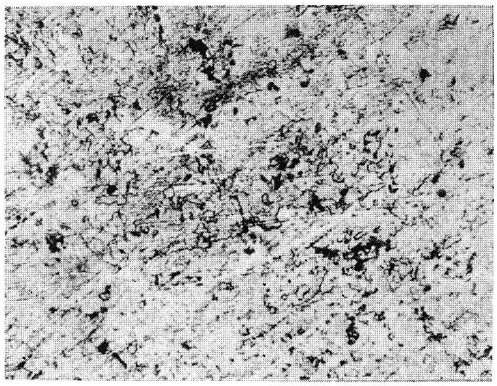

Duralumin D-26 (Cross Section) ×175

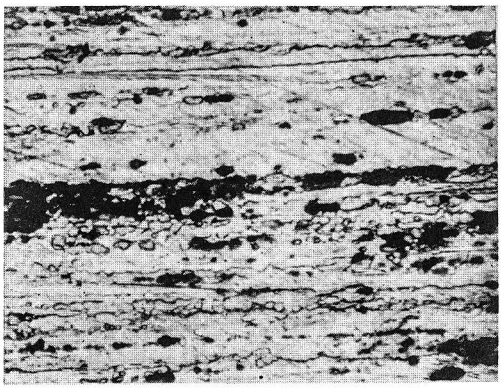

Duralumin D-26 (Longitudinal Section) ×175

Duralumin D-24 (Longitudinal Section) ×175

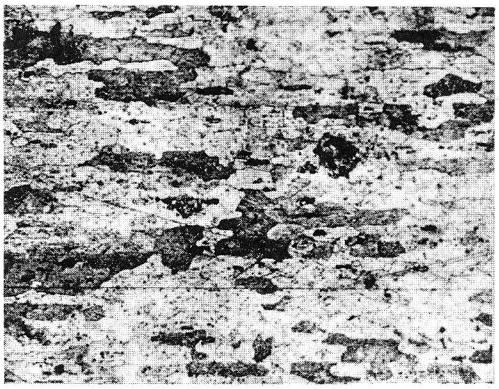

Duralumin D-24 (Longitudinal Section) ×175

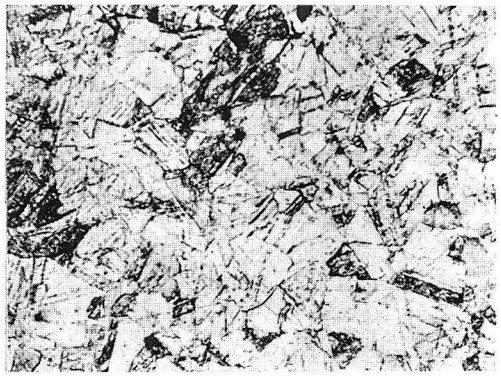

Brass (Cross Section) ×175

Fig. 6 (b). Microscopical Structures of Materials.

parts. Rotating bending fatigue tests were made to compare with the results obtained by combined stress fatigue tests.

The complete static tensile tests to destruction were made on two specimens of each material. The values of the results obtained are summarized in Table 2. In the tension tests of three carbon steels investigated here, yield points were clearly observed, but in other materials there was no marked drop of load at yield points, as in Fig. 8. Fig. 8 shows the load-elongation diagrams to fracture obtained by an autographic recorder in the tension tests. So that in the static tensile tests of the materials other than three carbon steels, strain measurements were made by means of a mirror extensometer of the Martens type, and from the stress-strain diagrams thus obtained, yield points were decided as the point of 0.2 per cent permanent set. Brinell hardness tests were made also on two specimens of each material, and the results are added in Table 2.

IV. Description of the Combined Stresses and the Test Results Obtained.

Owing to the inertia forces of fly wheel, a range of moment $\pm M$ is applied to the specimen. Then as previously mentioned, the specimen is subjected to bending and twisting moment equal to $M \sin\theta$ and $M \cos\theta$ respectively. The moments produce the following maximum direct and shearing stresses :

(a) Combined Stress Fatigue Specimen.

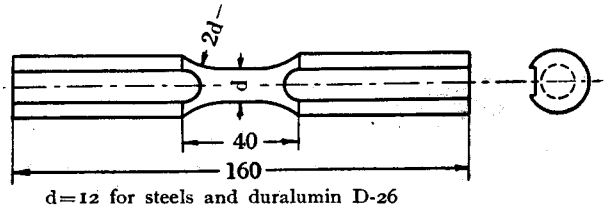

d=12 for steels and duralumin D-26
d=14 for duralumin D-24
d=15 for cast iron and brass

(b) Tensile Specimen

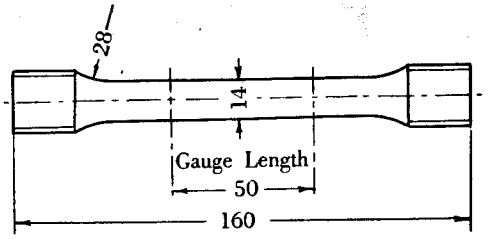

(c) Ono's Rotating Bending Fatigue Specimen.

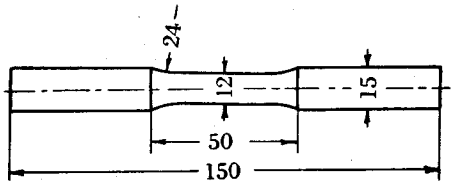

(d) Wöhler's Rotating Bending Fatigue Specimen.

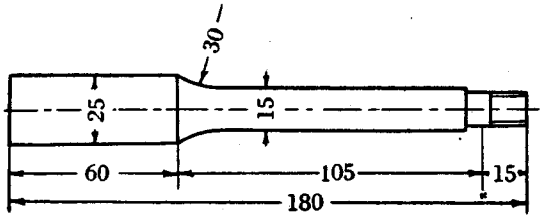

Fig. 7. Test Specimens.

Table 2. Heat Treatment and Mechanical Properties of Materials.

Materials	Hert Treatment	Upper Yield Point kg/mm²	Lower Yield Point kg/mm²	Ultimate Strength kg/mm²	Breaking Stress on Final Area kg/mm²	Elongation %	Reduction of Area %	Brinell* Hardness Number
Mild Steel	Annealed from 900 deg. C	31.9 28.0	23.3 23.0	38.4 38.3	84.5 89.4	— 49.4	71.4 72.9	104 103
Medium Steel	Annealed from 850 deg. C	29.8 29.7	28.7 28.5	53.3 52.9	83.7 78.7	31.5 30.5	45.4 44.8	134 132
Hard Steel	Normalized from 780 deg. C	36.3 37.2	35.5 36.5	71.3 72.5	97.8 100.4	23.5 24.0	32.8 32.6	187 201
Nsckel-Chromium Steel	Hot-rolled	51.3 47.0	— —	73.8 69.7	125.2 129.0	20.2 28.0	57.8 60.6	237 237
	Normalized from 900 deg. C, quenched from 850 deg. C, tempered for 40 min at 600 deg. C	91.5 87.7	— —	98.0 98.2	125.7 125.3	21.0 20.4	45.0 44.7	294 295
Cast Iron	Casted	— —	— —	22.6 21.3	— —	— —	— —	— —
Duralumin D-26	Extruded, quenched	33.1 33.8	— —	45.7 46.8	56.5	15 14	26.2	95.5 94.0
Duralumin D-24	Extruded, quenched	23.6 23.1	— —	38.6 38.0	59.0 —	25 25	39.8 —	84 86
Brass	Extruded	34.1 34.7	— —	42.3 41.1	103.3 101.5	40.6 44.4	70.5 70.2	123 121

Two specimens were tested for every material.

* Load was 3000 kg in steel and cast iron, 500 kg in duralumins, and 1000 kg in brass. Ball diameter was 10 mm.

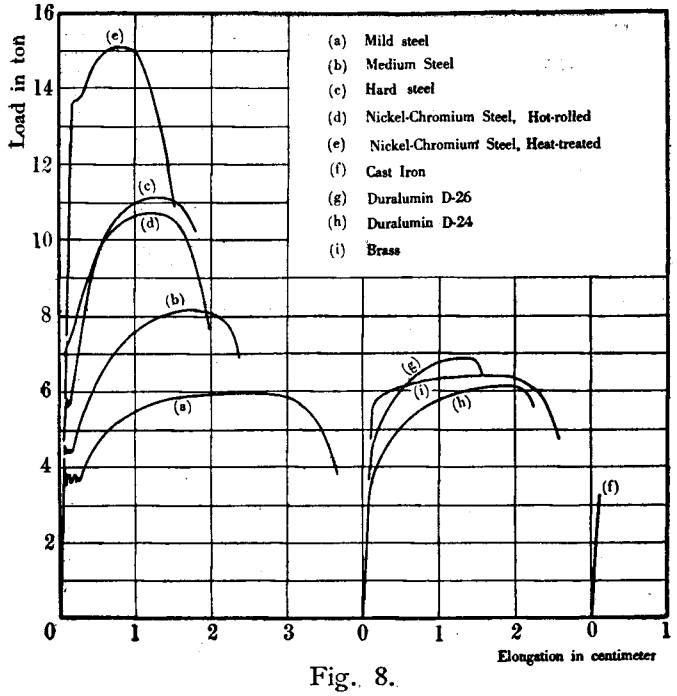

Fig. 8.
Autographic Tensile Load-Elongation Diagram.

Direct stress σ due to bending moment

$$= \frac{32}{\pi d^3} M \sin\theta$$

Shearing stress τ due to twisting moment

$$= \frac{16}{\pi d^3} M \cos\theta$$

where d is the diameter of the specimen. In the stress system induced here the maximum and minimum principal stresses, σ_{max}, σ_{min}, and the maximum shearing stress τ_{max} are as follows:

$$\sigma_{max} = \frac{1}{2}(\sqrt{\sigma^2+4\tau^2}+\sigma) = \frac{16}{\pi d^3} M(1+\sin\theta)$$

$$\sigma_{min} = \frac{1}{2}(\sqrt{\sigma^2+4\tau^2}-\sigma) = -\frac{16}{\pi d^3} M(1-\sin\theta)$$

$$\tau_{max} = \frac{1}{2}\sqrt{\sigma^2+4\tau^2} = \frac{16}{\pi d^3} M$$

and the direction of the plane of the maximum principal stress is inclined to the longitudinal axis of the specimen at an angle $\frac{1}{2}\tan^{-1}\frac{2\tau}{\sigma}$, which is equal to the angle $\frac{1}{2}\left(\frac{\pi}{2}-\theta\right)$.

When the diameter of the specimen is constant, the value of the maximum shear stress induced is proportional to the moment M, being independent of the angle θ. So it is convenient to use the maximum shear stress value instead of the moment M in expressing the results obtained in the combined fatigue stress experiments.

In the endurance tests described here, ten millions of stress cycles were always used to determine the fatigue limit, though it is desirable for the non-ferrous materials to apply much more stress cycles, such as a hundred million or more. But it is not necessary to apply so many stress cycles to know a criterion of fatigue failures of the material, because the criterion was found above a certain limit, to have no relation to the number of stress cycles applied.

The results of the experiments made in the combined stress machine are as follows:

(1) Mild steel. Fatigue limits were determined

Table 3.
Results of Combined Stress Fatigue Tests on Mild Steel.

No.	θ deg.	Maximum Shear Stress Induced by Combined Stresses, τ_{max} kg/mm²	Maximum Direct Stress due to Bending, σ kg/mm²	Maximum Shear Stress due to Torsion, τ kg/mm²	Number of Repetitions, N 10^6	Remarks
L19		19.0		19.0	0.189	Broken
L 3		18.0		18.0	0.408	"
L 4		17.0		17.0	0.584	"
L 5	0	16.0	0	16.0	0.724	"
L 9		15.5		15.5	5.396	"
L 6		15.0		15.0	10.596	"
L20		"		"	12.574	Unbroken
L15	22.5	18.0	13.8	16.6	0.172	Broken
L22		14.5	11.1	13.4	4.992	"
L16	45	14.5	20.5	10.25	4.336	Broken
L18		14.0	19.8	9.9	10.664	Unbroken
L17	67.5	15.0	27.7	5.74	1.560	Broken
L21		14.0	25.9	5.36	3.542	"
L10		17.0	34.0		0.189	Broken
L11		16.0	32.0		0.412	"
L12	90	15.0	30.0	0	0.584	"
L13		14.0	28.0		1.768	"
L14		13.5	27.0		10.992	Unbroken

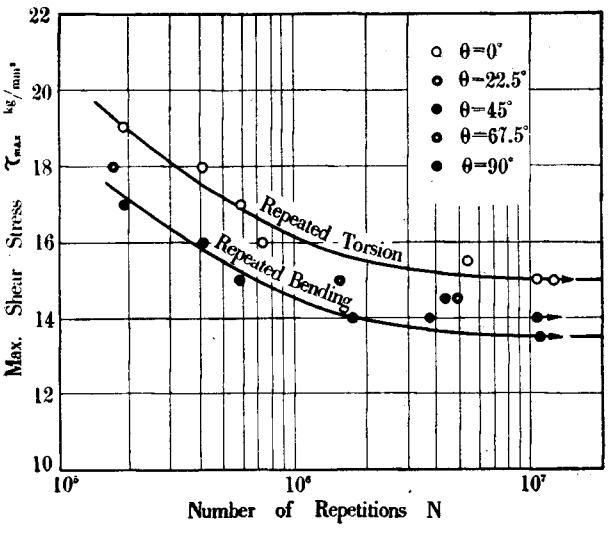

Fig. 9.
Stress-Endurance Curves for Mild Steel.

under three stress conditions, i. e. under reversed simple bending stresses, reversed simple torsional stresses, and a combination of these types of stressing action (at 45 degree of the angle θ). The results obtained are as given in Table 3, Fig. 9.

(2) Medium steel. In this case sufficient numbers of specimens and values of range of stress were used to determine the fatigue limit. Experiments were carried out under seven stress combinations, i.e. at the value of θ, 0, 15, 30, 45, 60, 75, and 90 degree. The results are shown in Table 4, Fig. 10.

Table 4.

Results of Combined Stress Fatigue Tests on Medium Steel.

No.	θ deg.	Maximum Shear Stress Induced by Combined Stresses, τ_{max} kg/mm²	Maximum Direct Stress due to Bending, σ kg/mm²	Maximum Shear Stress due to Torsion, τ kg/mm²	Number of Repetitions, N 10^6	Remarks
8		14.65		14.65	0.41	Broken
2	0	14.35	0	14.35	1.26	"
9		14.08		14.08	10.50	Unbroken
42		14.27	7.49	13.78	0.27	Broken
39	15	14.00	7.25	13.52	0.21	"
37		13.72	7.10	13.25	10.07	Unbroken
38		13.46	6.97	13.00	10.85	"
3		14.90	14.90	12.90	0.57	Broken
4		14.60	14.60	12.64	1.26	"
5		14.45	14.45	12.51	0.35	"
10	30	14.17	14.17	12.27	2.10	"
12		13.90	13.90	12.03	0.61	"
20		13.63	13.63	11.80	0.93	"
11		13.62	13.62	11.79	4.36	"
17		13.34	13.34	11.55	10.35	Unbroken
43		13.80	19.50	9.75	2.80	Broken
40	45	13.50	19.08	9.65	2.00	"
34		13.22	18.70	9.35	2.15	"
36		12.95	18.32	9.16	10.85	Unbroken
13		13.87	24.02	6.94	0.818	Broken
14		13.58	23.52	6.79	0.652	"
15		13.30	23.04	6.65	1.39	"
24	60	13.15	22.76	6.58	0.588	"
16		13.00	22.50	6.50	1.43	"
33		12.87	22.28	6.44	0.92	"
18		12.70	22.19	6.35	1.80	"
30		12.58	21.80	6.29	10.72	Unbroken
49		13.30	25.70	3.44	0.504	Broken
28	75	12.73	24.59	3.29	2.36	"
29		12.44	24.03	3.22	10.48	Unbroken
21		13.36	26.72		0.716	Broken
27	90	12.78	25.56	0	1.66	"
40		12.48	24.96		3.38	"
26		12.20	24.40		10.79	Unbroken

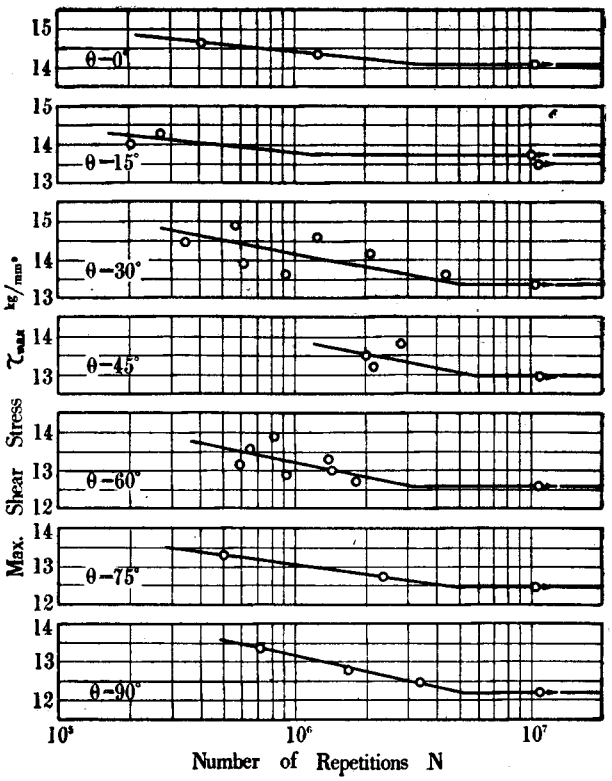

Fig. 10. Stress-Endurance Curves for Medium Steel.

(3) Hard steel. Tests were made in the same manner as in the case of medium steel. Results are given in Table 5, Fig. 11.

Table 5.

Results of Combined Stress Fatigue Tests on Hard Steel.

No.	θ deg.	Maximum Shear Stress Induced by Combined Stresses, τ_{max} kg/mm²	Maximum Direct Stress due to Bending, σ kg/mm²	Maximum Shear Stress due to Torsion, τ kg/mm²	Number of Repetitions, N 10^6	Remarks
H 3		22.0		22.0	0.45	Broken
H 9	0	21.0	0	21.0	1.28	"
H 4		20.0		20.0	10.55	Unbroken
H13		"		"	9.50	"
H15		19.5	10.10	18.83	3.12	Broken
H17	15	"	"	"	1.24	"
H14		18.5	9.58	17.87	10.23	Unbroken
H12	30	18.3	18.30	15.84	1.49	Broken
H23		17.3	17.30	14.95	10.64	Unbroken
H16	45	17.5	24.75	12.37	0.85	Broken
H18		16.5	23.33	11.66	10.25	Unbroken
H20	60	17.0	29.44	8.50	2.43	Broken
H10		16.0	27.70	8.00	13.94	Unbroken
H22	75°	16.0	30.90	4.14	3.47	Broken
H25		15.0	28.97	3.88	10.65	Unbroken
H 5	90°	16.0	32.0	0	1.54	Broken
H11		15.0	30.0		11.72	Unbroken

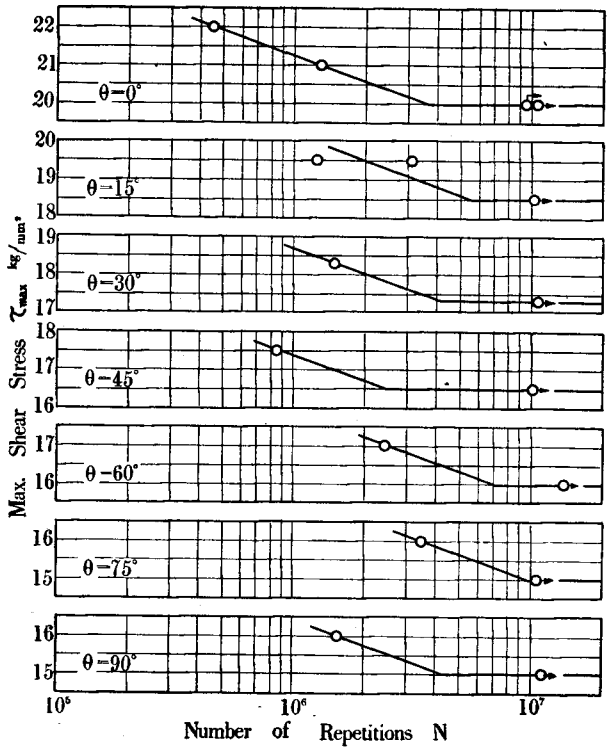

Fig. 11.
Stress-Endurance Curves for Hard Steel.

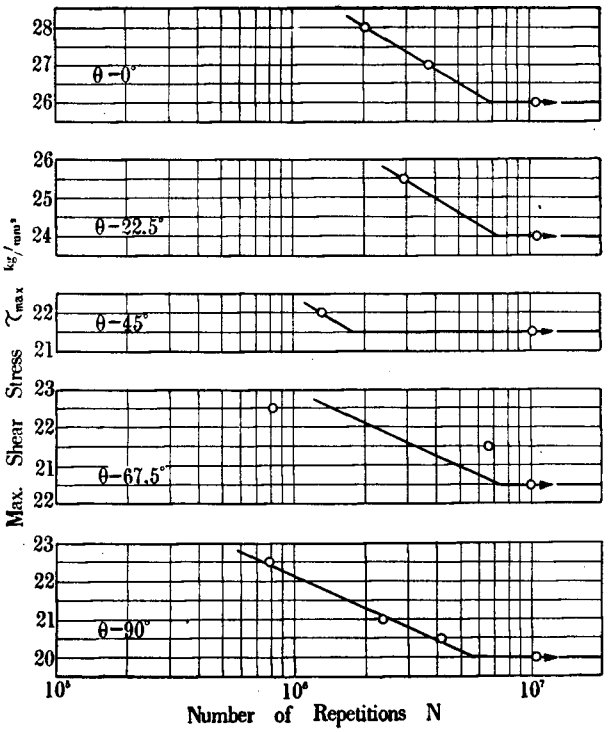

Fig. 12.
Stress-Endurance Curves for Hot-rolled Nickel-Chromium Steel.

(4) Nickel-chromium steel, hot-rolled. Tests were made under five stress combinations, i. e. at each of five values, 0, 22.5, 45, 67.5, and 90 deg., of the angle θ. The results are given in Table 6, Fig. 12.

Table 6.
Results of Combined Stress Fatigue Tests on Hot-rolled Nickel-Chromium Steel.

No.	θ deg.	Maximum Shear Stress Induced by Combined Stresses, τ_{max} kg/mm²	Maximum Direct Stress due to Bending, σ kg/mm²	Maximum Shear Stress due to Torsion, τ kg/mm²	Number of Repetitions, N 10^6	Remarks
N 6	0	28.0	0	28.0	2.04	Broken
N 8		27.0		27.0	3.76	"
N13		26.0		26.0	10.67	Unbroken
N 7	22.5	25.5	19.5	23.5	2.94	Broken
N16		24.0	18.4	22.2	10.76	Unbroken
N 9	45	22.0	31.1	15.6	1.32	Broken
N12		21.5	30.4	15.2	10.29	Unbroken
N11	67.5	22.5	41.6	8.62	0.816	Broken
N10		21.5	39.7	8.23	6.64	"
N15		20.5	37.9	7.85	10.05	Unbroken
N 3	90	22.5	45.0	0	0.79	Broken
N 4		21.0	42.0		2.39	"
N14		20.5	41.0		4.18	"
N 5		20.0	40.0		10.48	Unbroken

(5) Nickel-chromium steel, heat-trea ed. Tests were made in the same manner as in the case of nickel-chromium steel, hot-rolled. Table 7, Fig. 13 shows the results obtained.

Table 7.
Results of Combined Stress Fatigue Tests on Heat-treated Nickel-Chromium Steel.

No.	θ deg.	Maximum Shear Stress Induced by Combined Stresses, τ_{max} kg/mm²	Maximum Direct Stress due to Bending, σ kg/mm²	Maximum Shear Stress due to Torsion, τ kg/mm²	Number of Repetitions, N 10^6	Remarks
NT 3	0	35	0	35	0.444	Broken
NT 4		33		33	0.736	"
NT22		32		32	3.860	"
NT 6		31		31	10.917	Unbroken
NT 9	22.5	33	25.3	30.5	2.900	Broken
NT19		32	24.5	29.6	3.132	"
NT 8		31	23.7	28.6	11.630	Unbroken
NT12	45	30	42.4	21.2	0.192	Broken
NT13		29	41.0	20.5	3.096	"
NT21		28	39.6	19.8	10.543	Unbroken
NT14	67.5	29	53.6	11.1	0 132	Broken
NT15		28	51.7	10.7	0.420	"
NT16		27	49.9	10.3	14.487	Unbroken
NT10	90	29	58	0	0.296	Broken
NT 7		28	56		3.810	"
NT11		27	54		11.300	Unbroken

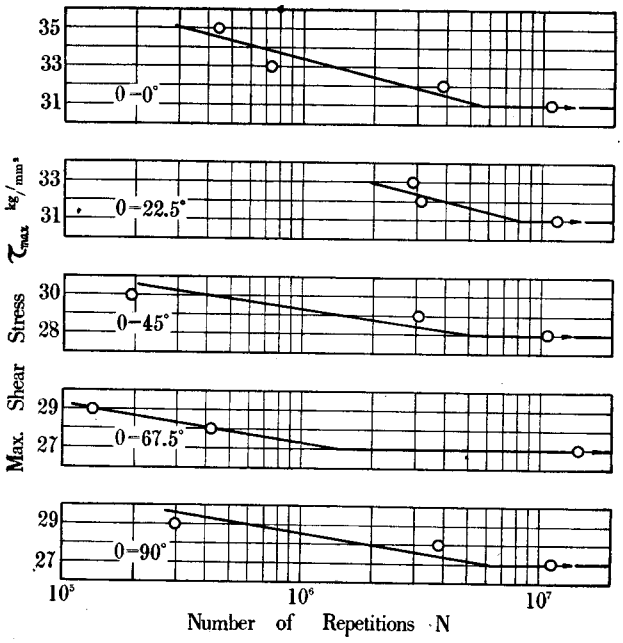

Fig. 13.
Stress-Endurance Curves for Heat-treated Nickel-Chromium Steel.

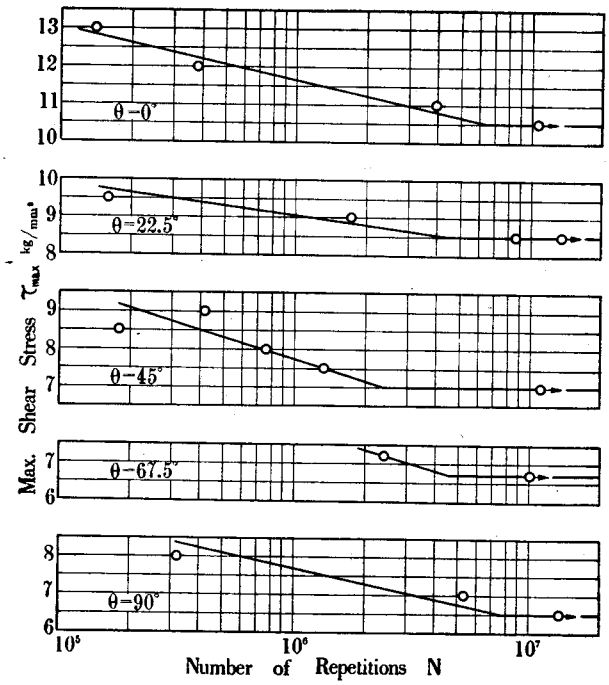

Fig. 14.
Stress-Endurance Curves for Cast Iron.

(6) Cast iron. Tests were made in the same manner as in the case of nickel-chromium steel. Table 8, Fig. 14 shows the results obtained.

Table 8.

Results of Combined Stress Fatigue Tests on Cast Iron.

No.	θ deg.	Maximum Shear Stress Induced by Combined Stresses, τ_{max} kg/mm²	Maximum Direct Stress due to Bending, σ kg/mm²	Maximum Shear Stress due to Torsion, τ kg/mm²	Number of Repetitions, N 10^6	Remarks
0	0	13.0	0	13.0	0.14	Broken
1		12.0		12.0	0.38	,,
4		11.0		11.0	3.94	,,
5		10.5		10.5	10.65	Unbroken
14	22.5	9.5	7.26	8.78	0.16	Broken
15		9.0	6.88	8.32	1.73	,,
16		8.5	6.50	7.85	8.67	,,
19		,,	,,	,,	13.48	Unbroken
8	45°	9.0	12.72	6.36	0.42	Broken
9		8.5	12.02	6.01	0.18	,,
10		8.0	11.32	5.66	0.76	,,
12		7.5	10.60	5.30	1.33	,,
11		7.0	9.90	4.95	11.15	Unbroken
17	67.5°	7.2	13.30	2.75	2.43	Broken
18		6.7	12.38	2.56	10.06	Unbroken
6	90°	8.0	16.0	0	0.22	Broken
7		7.0	14.0		5.34	,,
13		6.5	13.0		13.54	Unbroken

(7) Duralumin D-26. Seven stress combinations were adopted in this case. Table 9, Fig. 15 shows the test results.

Table 9.

Results of Combined Stress Fatigue Tests on Duralumin D-26.

No.	θ deg.	Maximum Shear Stress Induced by Combined Stresses, τ_{max} kg/mm²	Maximum Direct Stress due to Bending, σ kg/mm²	Maximum Shear Stress due to Torsion, τ kg/mm²	Number of Repetitions, N 10^6	Remarks
14	0	9.0	0	9.0	0.72	Broken
2		8.5		8.5	1.29	,,
3		8.0		8.0	4.01	,,
4		7.5		7.5	12.08	Unbroken
16	15	8.5	4.30	8.21	0.86	Broken
7		8.0	4.14	7.73	8.25	,,
5		7.5	3.88	7.24	10.04	Unbroken
18	30	8.5	8.50	7.36	2.16	Broken
9		8.0	8.00	6.93	5.34	,,
6		7.5	7.50	6.49	10.10	Unbroken
20	45	8.0	11.31	5.66	2.36	Broken
17		7.5	10.60	5.30	12.80	Unbroken
19	60	8.0	13.85	4.00	2.68	Broken
15		7.5	12.98	3.75	11.08	Unbroken
11	75	8.0	15.45	2.07	3.47	Broken
12		7.5	14.48	1.94	10.03	Unbroken
21	90	8.5	17.0	0	1.85	Broken
13		8.0	16.0		6.08	,,
10		7.5	15.0		10.83	Unbroken

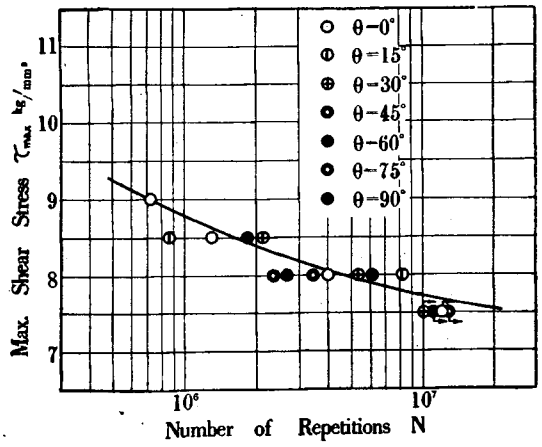

Fig. 15.
Stress-Endurance Curves for Duralumin D-26.

(8) Duralumin D-24. Tests were made under three stress combinations as in the case of mild steel. To see the fatigue failure, some specimens were broken at each of two values, 22.5 and 67.5 deg., of the angle θ. The results are shown in Table 10, Fig. 16.

(9) Brass. Tests were made under five stress combinations. The results are shown in Table 11, Fig. 17. In this case fatigue limits for 10^7 stress repetitions are estimated by the stress-endurance curve.

In these tables, applied stresses are mentioned in the calculated values of the direct and shear stresses due to bending and twisting moments respectively, and also of the maximum shear stresses

Table 10.
Results of Combined Stress Fatigue Tests on Duralumin D-24.

No.	θ deg.	Maximum Shear Stress Induced by Combined Stresses, τ_{max} kg/mm²	Maximum Direct Stress due to Bending, σ kg/mm²	Maximum Shear Stress due to Torsion, τ kg/mm²	Number of Repetitions, N 10^6	Remarks
d 1		20.0		20.0	0.019	Broken
d 2		18.0		18.0	0.044	"
d 3		16.0		16.0	0.046	"
d 8		14.0		14.0	0.208	"
d 9	0	12.0	0	12.0	1.272	"
d 12		11.0		11.0	1.704	"
d 18		9.5		9.5	2.748	"
d 19		9.0		9.0	6.530	"
d 24		8.5		8.5	10.013	Unbroken
d 22	22.5	14.0	10.7	12.9	0.152	Broken
d 21		18.0	25.5	12.7	0.017	Broken
d 20	45	8.5	12.0	6.0	8.635	"
d 23		8.0	11.3	5.7	10.024	Unbroken
d 25	67.5	14.0	25.9	5.4	0.077	Broken
d 5		16.0	32.0		0.020	Broken
d 6		14.0	28.0		0.048	"
d 7		12.0	24.0		0.368	"
d 11		11.0	22.0		0.249	"
d 14	90	10.0	20.0	0	0.428	"
d 15		9.0	18.0		1.587	"
d 13		8.5	17.0		3.608	"
d 16		8.0	16.0		3.464	"
d 17		7.5	15.0		10.152	Unbroken

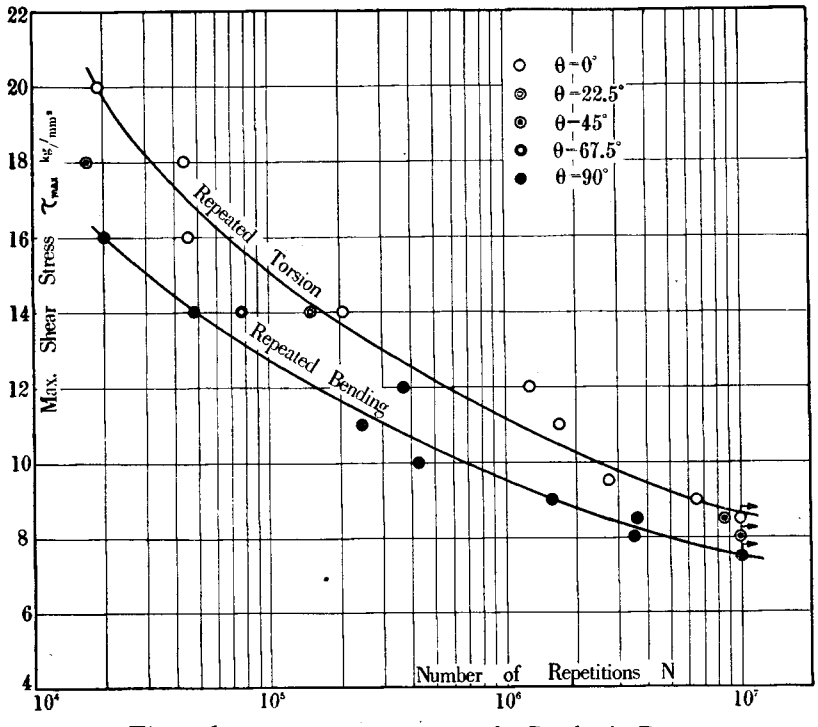

Fig. 16. Stress-Endurance Curves for Duralumin D-24.

Table 11.
Results of Combined Stress Fatigue Tests on Brass.

No.	θ deg.	Maximum Shear Stress Induced by Combined Stresses, τ_{max} kg/mm²	Maximum Direct Stress due to Bending, σ kg/mm²	Maximum Shear Stress due to Torsion, τ kg/mm²	Number of Repetitions, N 10^6	Remarks
25		15.0		15.0	0.292	Broken
5		11.5		11.5	1.036	,,
1		10.0		10.0	2.028	,,
4		9.5		9.5	2.888	,,
9	0	9.0	0	9.0	2.576	,,
10		8.5		8.5	3.812	,,
11		8.0		8.0	3.480	,,
12		7.5		7.5	5.638	,,
13		6.5		6.5	9.734	,,
17		11.5	8.8	10.63	0.772	,,
19	22.5	10.5	8.04	9.7	1.004	,,
21		8.5	6.5	7.85	3.060	,,
23		14.0	19.8	9.9	0.322	,,
7	45	9.5	13.4	6.7	2.744	,,
8		9.0	12.7	6.37	2.412	,,
20		13.0	24.0	4.97	0.399	,,
18	67.5	10.5	19.4	4.02	1.680	,,
22		8.5	15.7	3.25	3.368	,,
24		15.5	31.0		0.172	,,
16		10.5	21.0		1.830	,,
2	90	9.5	19.0	0	2.060	,,
15		8.0	16.0		5.582	,,
14		6.5	13.0		12.339	Unbroken

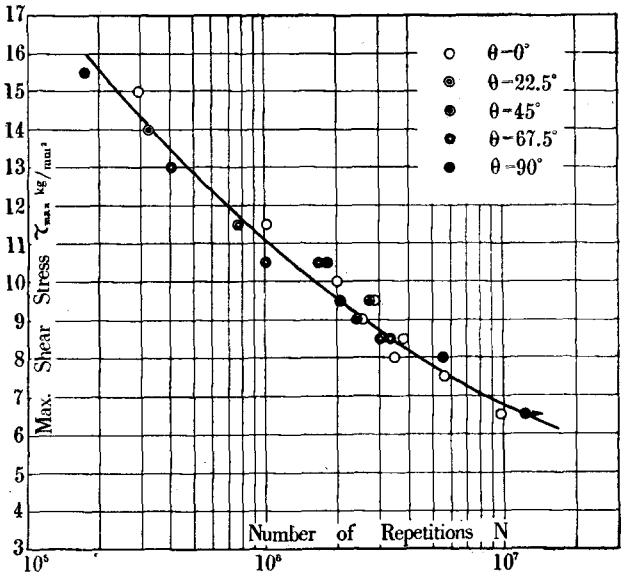

Fig. 17.
Stress-Endurance Curves for Brass.

induced in specimens. Stress-endurance curves show the relation of the maximum shear stress and number of cycles applied.

V. Consideration of Experimental Results.

In examining the results obtained for each material, it is convenient to show these results in diagrams, having the direct stress due to bending in abscissa and the shearing stress due to torsion in ordinate, that is, in $\sigma-\tau$ diagrams. Figs. 18–26 show the $\sigma-\tau$ diagrams of each material. In these

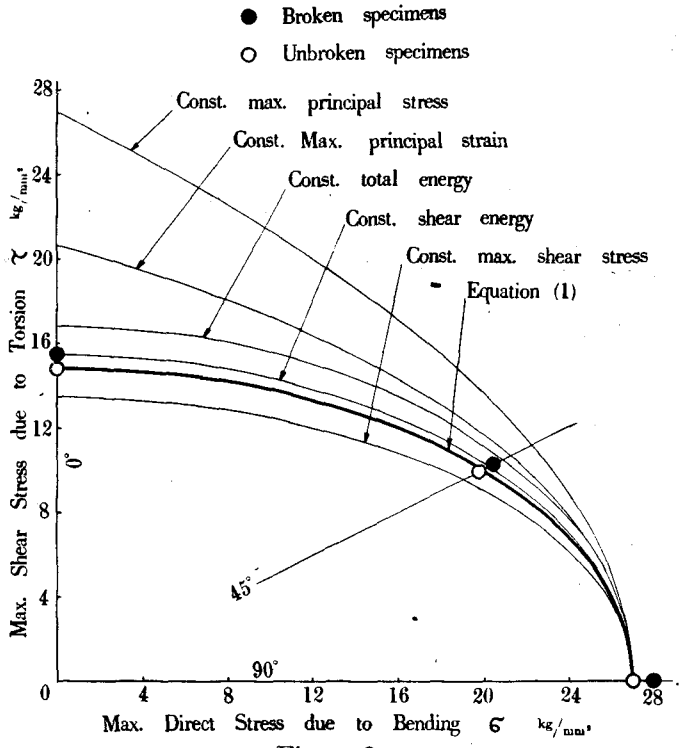

Fig. 18.
$\sigma-\tau$ Diagram for Mild Steel.

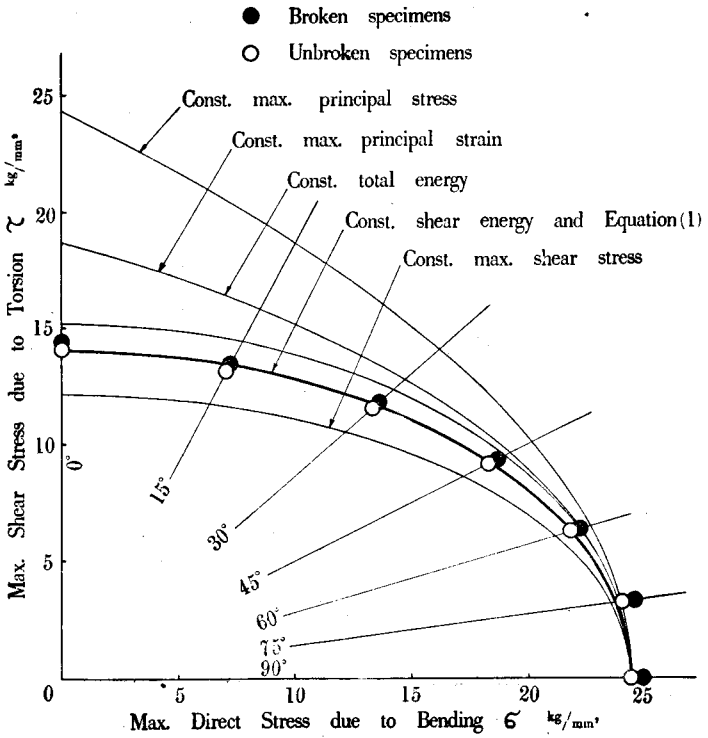

Fig. 19.

$\sigma-\tau$ Diagram for Medium Steel.

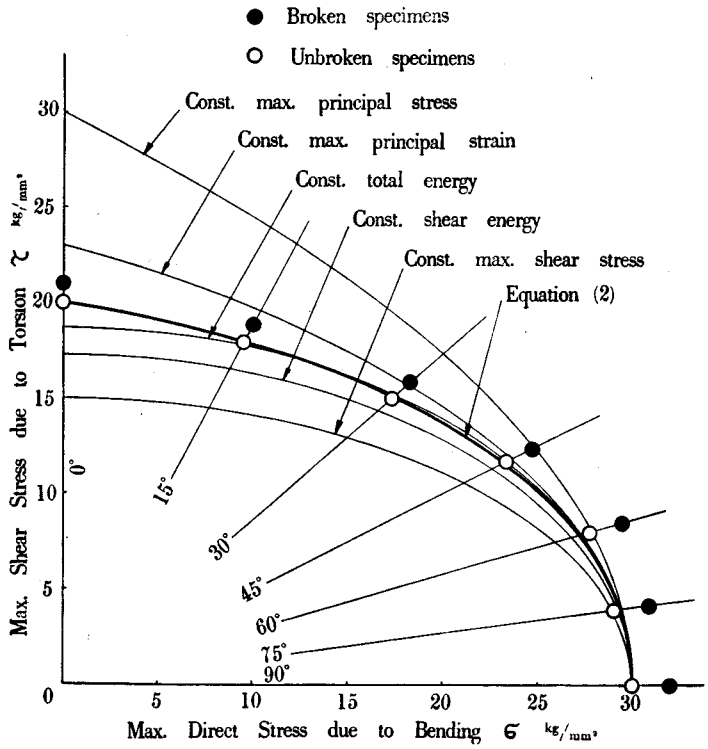

Fig. 20.

$\sigma-\tau$ Diagram for Hard Steel.

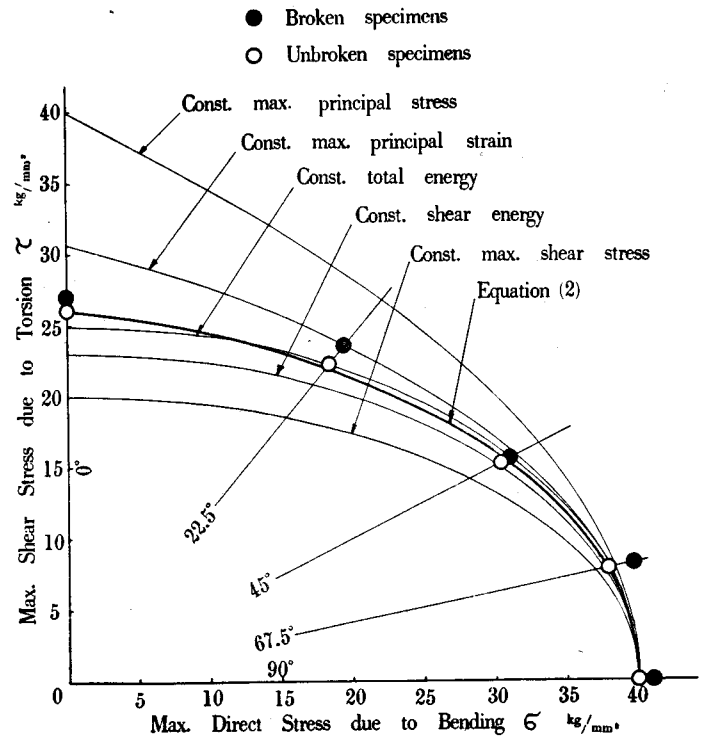

Fig. 21.

$\sigma-\tau$ Diagram for Hot-rolled Nickel-Chromium Steel.

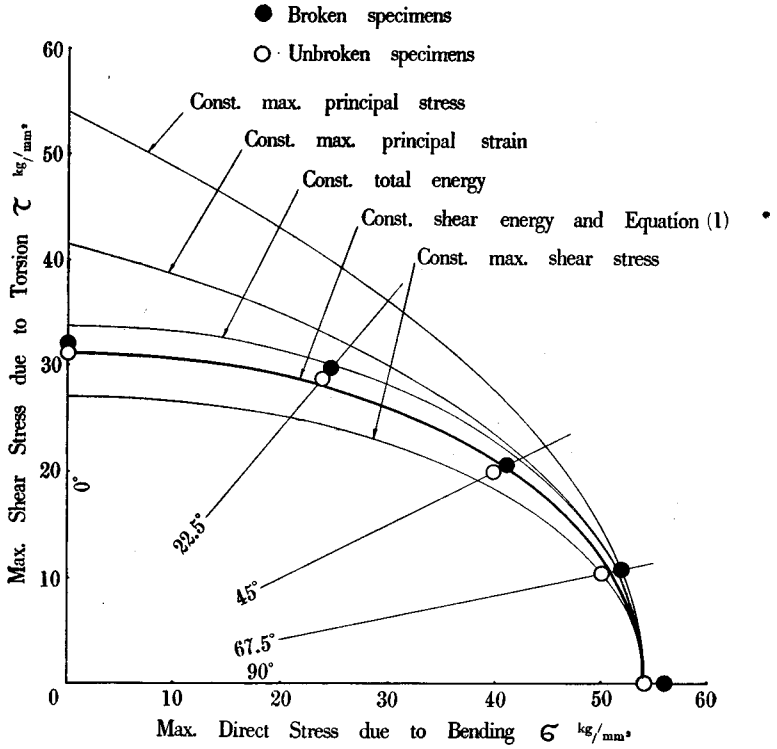

Fig. 22.

$\sigma-\tau$ Diagram for Heat-treated Nickel-Chromium Steel.

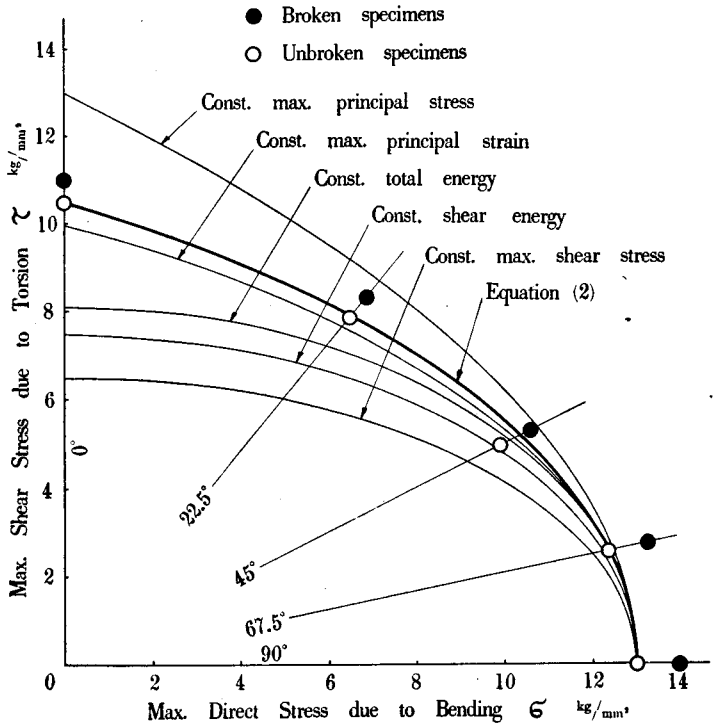

Fig. 23.

$\sigma-\tau$ Diagram for Cast Iron.

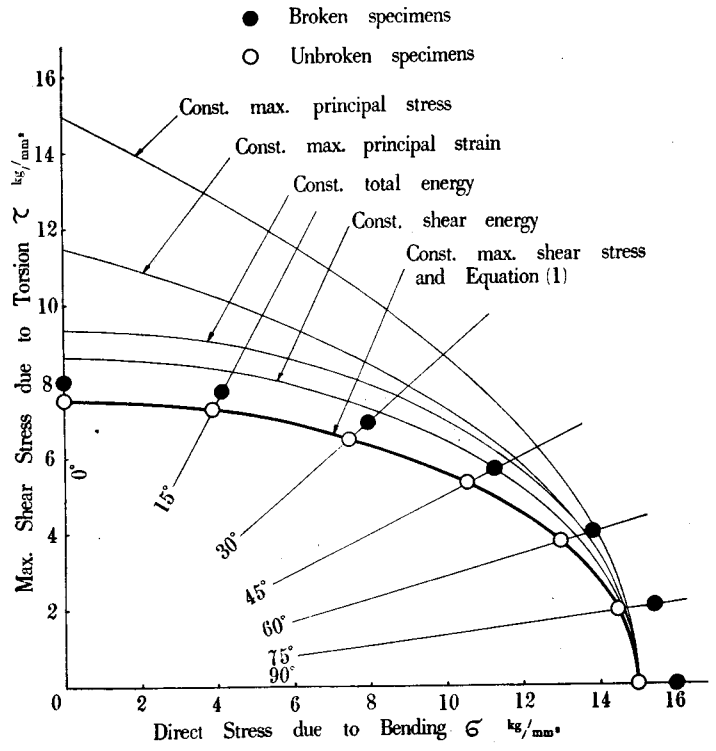

Fig. 24.

$\sigma-\tau$ Diagram for Duralumin D-26.

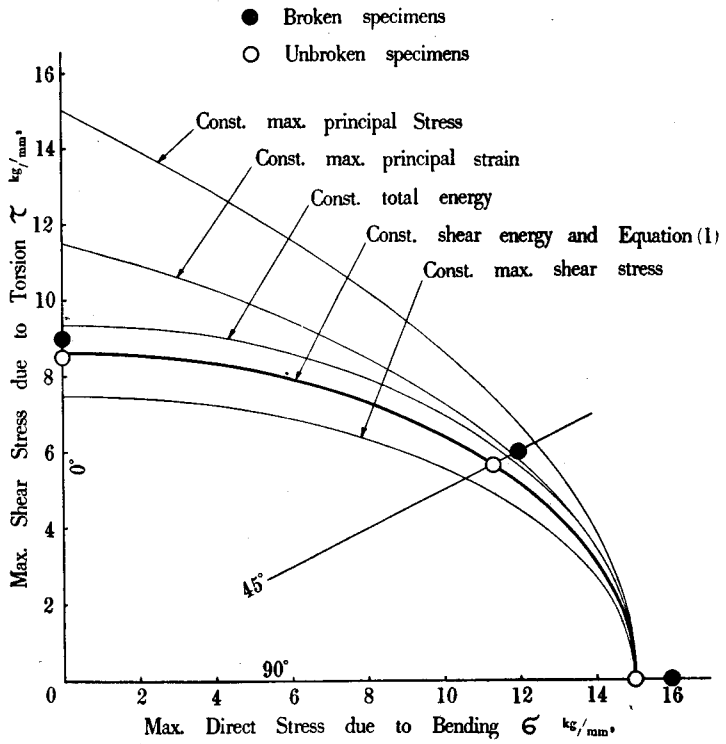

Fig. 25.

$\sigma-\tau$ Diagram for Duralumin D-24.

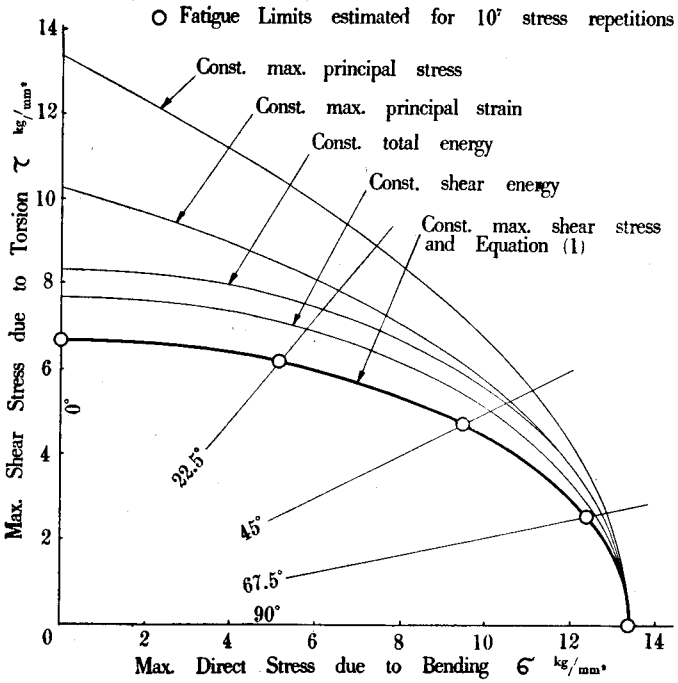

Fig. 26.

$\sigma-\tau$ Diagram for Brass.

diagrams the results of reversed bending ($\theta=90$ deg.) and reversed torsion ($\theta=0$ deg.) are plotted respectively on σ and τ axis, while the results of combined bending and torsion, having any value of the angle θ, are plotted on a radial line which has an included angle $\tan^{-1}(2\tan\theta)$ with τ axis.

It is interesting to compare these results with some of the theories concerning the elastic failure of metals under static stresses. Applying these theories to the case considered here, the following relations are obtained:

Let

σ_w = fatigue limit in reversed bending

σ = maximum direct stress due to bending
τ = maximum shear stress due to torsion
at the fatigue limit of the combination

m = Poisson's constant

(1) Theory of constant maximum shear stress

$$\sigma^2+4\tau^2=\sigma_w^2$$

(2) Theory of constant maximum principal stress

$$\tau^2=\sigma_w(\sigma_w-\sigma)$$

(3) Theory of constant maximum principal strain

$$\left(\sigma+\frac{m-1}{2}\sigma_w\right)^2+\frac{(m+1)^2}{m}\tau^2=\frac{(m+1)^2}{4}\sigma_w^2$$

(4) Theory of constant total energy

$$\sigma^2+2\frac{m+1}{m}\tau^2=\sigma_w^2$$

(5) Theory of constant maximum shear energy

$$\sigma^2+3\tau^2=\sigma_w^2$$

The curves representing these equations are ellipses and parobola and added in Figs. 18–26 for purposes of comparison. The principal strain and total energy theories necessarily involve the value of Poisson's constant m. Though the value of m is different for each material, it was assumed here to be approximately 10/3 for all materials under consideration, because the shape of the curves representing those theories are not very sensitive to small changes in m.

Inspecting Figs. 18–26, it was cleared that the duralumin D-26 and the brass are in close accordance with the theory of constant maximum shear stress, while the medium steel, the heat-treated nickel-chromium steel and the duralumin D-24 conform closely to the theory of constant shear energy, which can also be applied to the mild steel with reasonable agreement. But none of the theory is applicable to the fatigue strength of the hard steel and the hot-rolled nickel-chromium steel. At the beginning of the tests of cast iron, the authors were much concerned about the irregularity of results, because cast iron is regarded as being usually subject to variations of strength from sample to sample. Nevertheless the results of cast iron were fairly regular and very satisfactory, but not consistent with any of the theories mentioned above. It seems to be anomalous that the results of duralumins D-26 and D-24 are consistent with different theories for each other. But it must be noted that, though both duralumins have nearly the same chemical compositions as in Table 1, duralumin D-26 seems to be received the effect of extrusion to the highest degree and has an extraordinary high static tensile strength, while duralumin D-24 has normal values of mechanical properties as shown in Table 2.

Results of hard steel, hot-rolled nickel-chromium steel, and cast iron are not in agreement with any theories. So from the engineering standpoint, it is desirable to establish a new criterion which is agreeable to all test results.

With regard to the mild steel, medium steel, heat-treated nickel-chromium steel, brass, and the two kinds of duralumins, the results of combined stress fatigue experiments can be expressed by the following ellipse with fair agreement:

$$\frac{\sigma^2}{\sigma_w^2}+\frac{\tau^2}{\tau_w^2}=1 \quad \text{or} \quad \sigma^2+\frac{1}{\varphi^2}\tau^2=\sigma_w^2 \qquad (1)$$

where

σ_w = fatigue limit in pure plane bending

τ_w = " " " " torsion

$\varphi=\tau_w/\sigma_w$

The values of σ_w, τ_w and φ in the present experiments were as follows:

	σ_w	τ_w	φ
Mild steel	27.0 kg/mm²	15.0 kg/mm²	0.556
Medium steel	24.4 "	14.08 "	0.577
Nickel-chromium steel, heat-treated	54.0 "	31.0 "	0.574
Duralumin D-26	15.0 "	7.5 "	0.500
Duralumin D-24	15.0 "	8.5 "	0.566
Brass	13.4 "	6.7 "	0.500

Applying these values in equation (1), elliptic relations between σ and τ can be obtained for each material, and these ellipses are drawn with thick lines in Figs. 18, 19, 22, 24, 25, 26.

Whereas as for the hard steel, hot-rolled nickel-chromium steel, and cast iron, the relation as in equation (1) cannot be applied without considerable error. Then authors propose to adopt the following expressions for these materials:

$$\left.\begin{aligned}&(\sigma_w^2-\tau_w^2)\sigma^2+(3\tau_w^2-\sigma_w^2)\sigma_w\sigma+2\sigma_w^2\tau^2=2\tau_w^2\\ \text{or}\quad&(1-\varphi^2)\sigma^2+(3\varphi^2-1)\sigma_w\sigma+2\tau^2=2\varphi^2\sigma_w^2\end{aligned}\right\} \qquad (2)$$

This equation is reduced to the expression corresponding to the theory of constant shear strain energy when φ is $1/\sqrt{3}$, and also to the theory of constant maximum principal stress when φ is 1. The value of σ_w, and τ_w, add φ obtained for these three materials were as follows:

	σ_w	τ_w	φ
Hard steel	30.0 kg/mm²	20.0 kg/mm²	0.667
Nickel-chromium steel, hot-rolled	40.0 "	26.0 "	0.650
Cast iron	13.0 "	10.5 "	0.808

Applying these values in equation (2), the curves drawn with thick lines in Figs. 20, 21, 23 are obtained. These curves are in very good agreement with the test results. Fig. 27 shows how the test results are in better agreement with the curve obtained with the equation (2) than with the ellipse or parabola, which is drawn to pass the two points corresponding to σ_w or τ_w respectively.

It will be concluded that the fatigue strength under combined bending and torsion can be obtained with the following expressions by determining values of σ_w and τ_w experimentally:

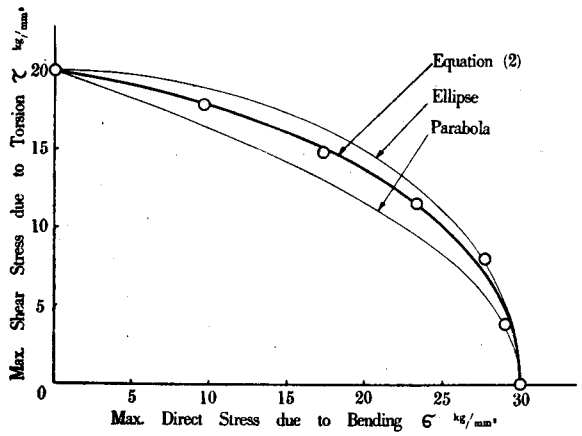

Fig. 27 (a).
Comparison of Equation (2) with Ellipse and Parabola.
Hard Steel.

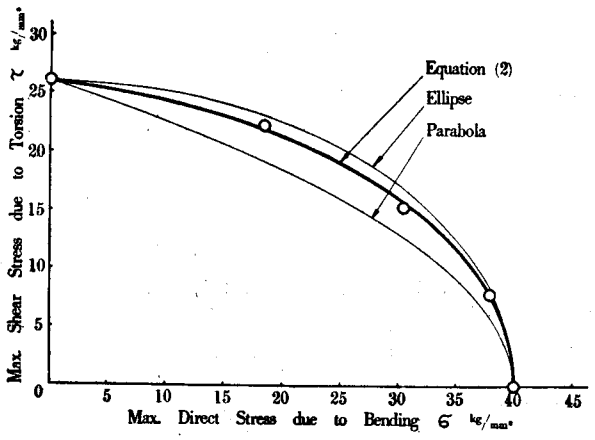

Fig. 27 (b).
Comparison of Equation (2) with Ellipse and Parabola.
Hot-rolled Nickel-Chromium Steel.

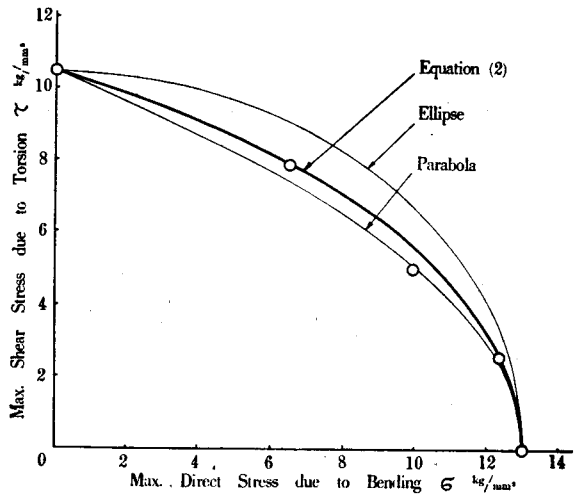

Fig. 27 (c).
Comparison of Equation (2) with Ellipse and Parabola.
Cast Iron.

$$\left.\begin{aligned} &\sigma^2+\frac{1}{\varphi^2}\tau^2=\sigma_w^2 \quad \text{for} \quad \varphi<\frac{1}{\sqrt{3}} \\ &(1-\varphi^2)\sigma^2+(3\varphi^2-1)\sigma_w\sigma+2\tau^2=2\varphi^2\sigma_w^2 \quad \text{for} \quad \varphi>\frac{1}{\sqrt{3}} \end{aligned}\right\} \tag{3}$$

In these equations, as previously mentioned, σ_w and τ_w are fatigue limits under pure bending and pure torsion respectively. For nonferrous metals, however, there exists no limiting range of stress which is just insufficient to cause fracture of materials under an indefinitely great number of applications of the particular stress cycles employed. So we can estimate a fatigue limit only for a certain limited number of stress cycles defined. The values of σ_w and τ_w for duralumins and brass above mensioned, were those for stress cycles of ten millions. For these nonferrous metals it is considered as an essential matter to confirm whether the relations expressed by equation (3) are applicable or not, when a different number of stress cycles is adopted to determine fatigue limits. To inquire about this subject, many specimens were tested for duralumin D-24 and brass under pure bending and pure torsion, to draw the so-called stress-endurance curves over wide ranges of number of stress cycles to fracture, as shown in Figs. 16 and 17 respectively. Experiments were made in a similar manner for mild steel as shown in Fig. 9, though in this case, fatigue limits for

Table 12.
Fatigue Limits for Different Numbers of Stress Cycles.

Materials	Fatigue Limits for Bending σ_w in kg/mm²			Fatigue Limits for Torsion τ_w in kg/mm²			$\frac{\tau_w}{\sigma_w}$		
	$N=10^5$	$N=10^6$	$N=10^7$	$N=10^5$	$N=10^6$	$N=10^7$	$N=10^5$	$N=10^6$	$N=10^7$
Duralumin D-24	25.9	19.1	15.0	15.1	11.2	8.7	0.583	0.587	0.580
Brass	—	22.2	13.6	—	11.1	6.8	—	0.500	0.500
Mild Steel	—	29.1	27.0	—	16.15	15.0	—	0.555	0.556

an indefinitely great number of stress cycles should be obtained.

Fatigue strength obtained for the duralumin D-24, the brass and the mild steel from the stress-endurance curves in Figs. 16, 17 and 8 is shown in Table 12, and Fig. 28 (a) (b) (c) shows these

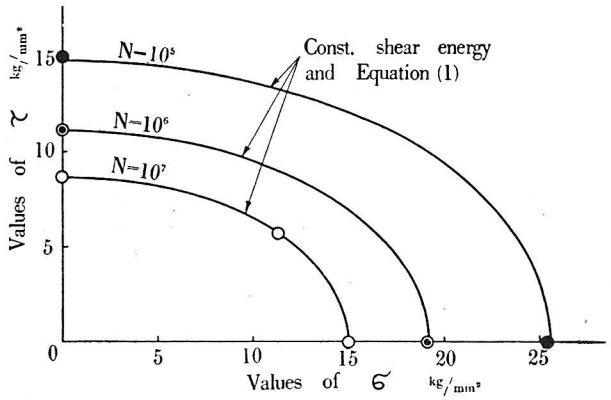

Fig. 28 (a).
Fatigue Limits for Different Numbers of Stres Cycles.
Duralumin D-24

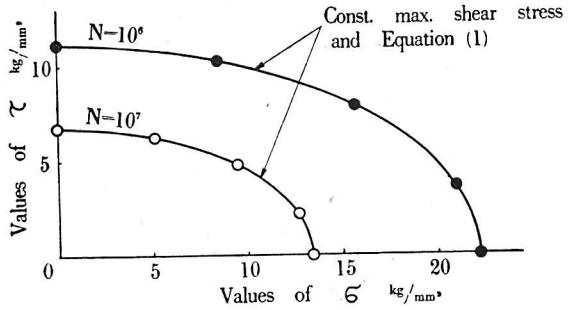

Fig. 28 (b).
Fatigue Limits for Different Numbers of Stress Cycles.
Brass.

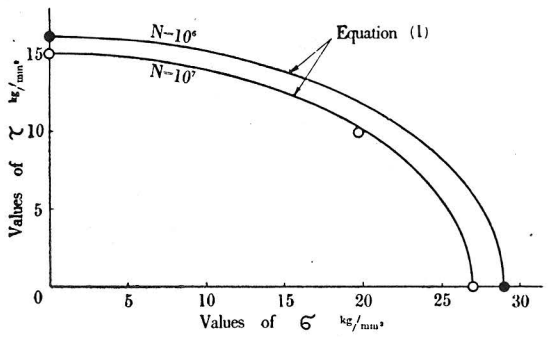

Fig. 28 (c).
Fatigue Limits for Different Numbers of Stres Cycles.
Mild Steel

relations in $\sigma-\tau$ diagrams. From these figures an important relation can be deduced, that the value of φ is always constant for each material and equation (3) is applicable for all materials, independent of the number of stress cycles defined, to determine the fatigue strength. Therefore it can be seen that no modification may be necessary for criteria of fatigue failures, even if experiments were made to a hundred million or more stress cycles for nonferrous metals.

VI. Fatigue Fractures.

In the combined stress fatigue tests, it is a very interesting and effective measure for investigation of fatigue mechanism to know the relation between the profile of fatigue failure and the combined stress condition applied. The fatigue fractures of all specimens which failed in the present experiments were observed minutely, and the following comparatively regular and informative results were obtained :

Mild Steel

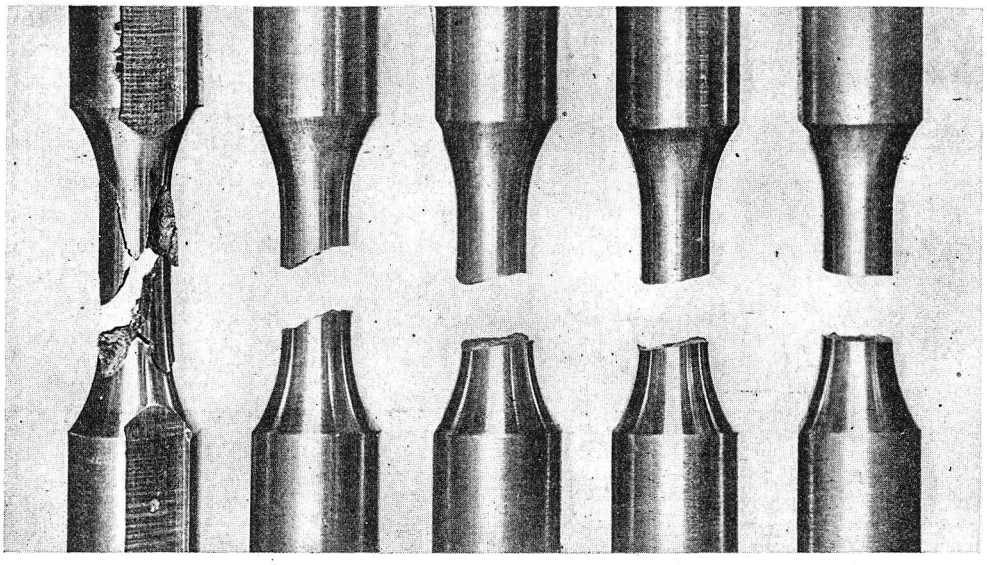

Fig. 29 (a). Fatigue Fractures of Carbon Steels.

Medium Steel

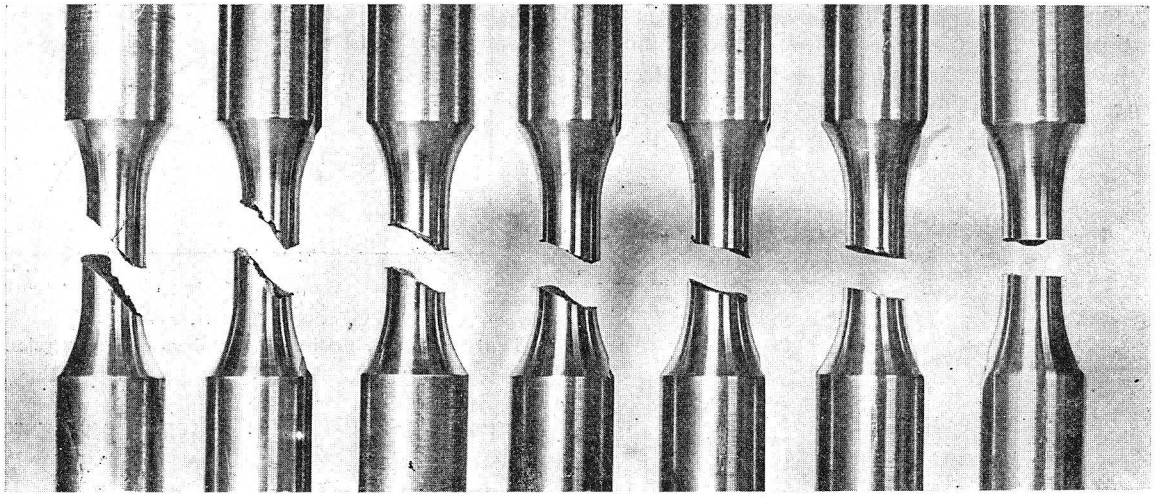

$\theta=0°$ $\theta=15°$ $\theta=30°$ $\theta=45°$ $\theta=90°$ $\theta=75°$ $\theta=90°$

Hard Steel

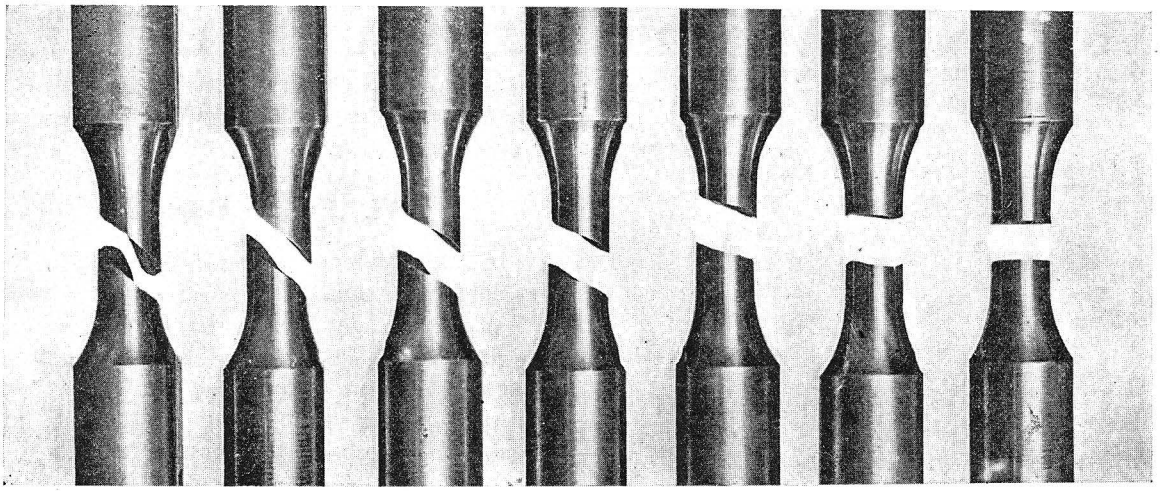

$\theta=0°$ $\theta=15°$ $\theta=30°$ $\theta=45°$ $\theta=60°$ $\theta=75°$ $\theta=90°$

Cast Iron.

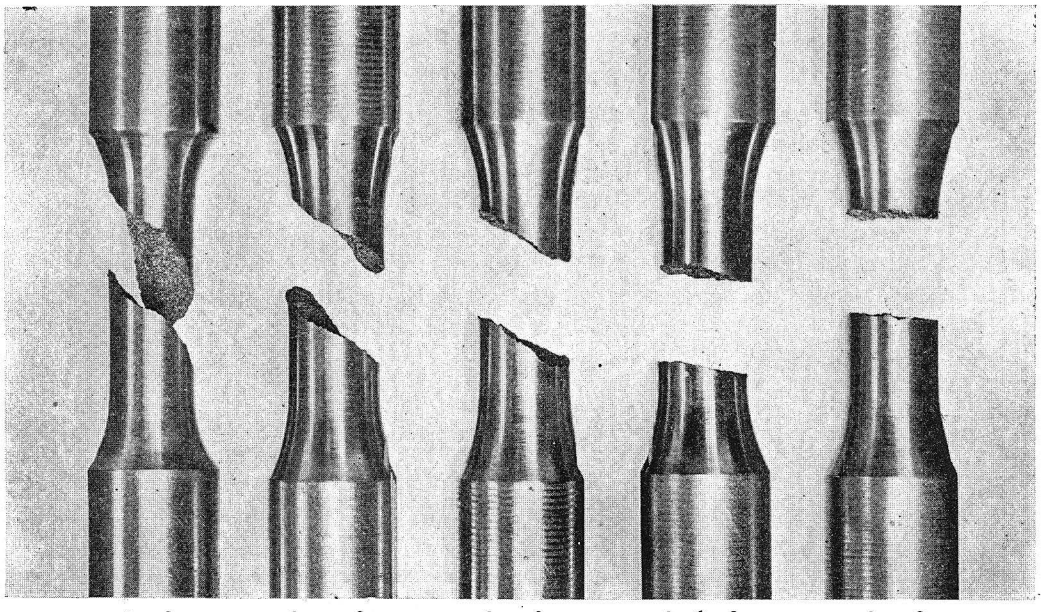

$\theta=0°$ $\theta=22.5°$ $\theta=45°$ $\theta=67.5°$ $\theta=90°$

Fig. 29 (b). Fatigue Fractures of Carbon Steels and Cast Iron.

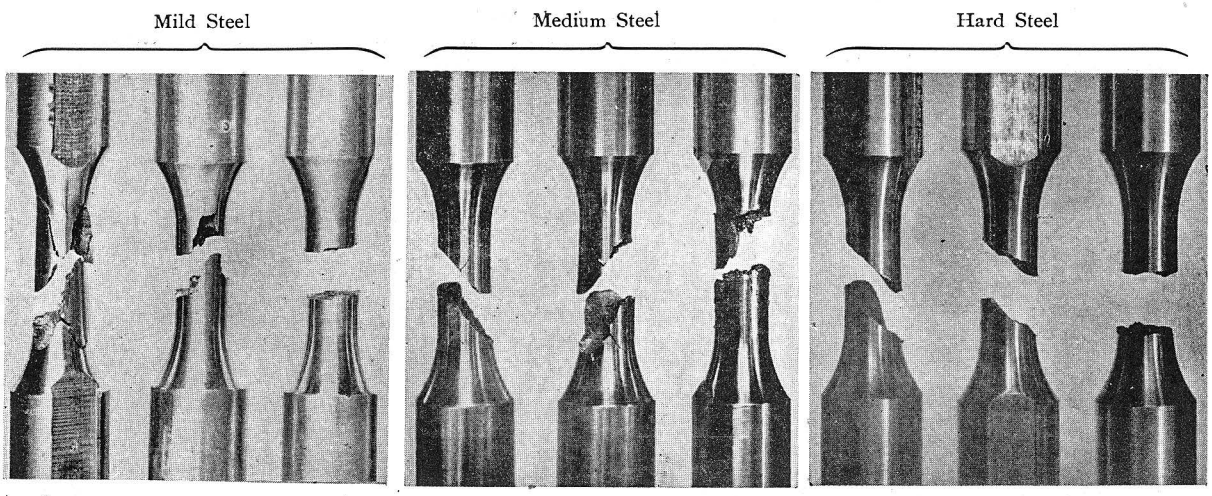

τ in kg/mm^2= 15,	15.5,	16,	14.35,	17,	20,	20,	22,	24
N in 10^6= 10.596,	5.396,	0.724,	1.26,	0.088,	0.018,	1.283,	0.121,	0.075

Fig. 30. Torsional Fatigue Fractures of Carbon Steels at Various Shear Stresses.

(*1*) *Fractures of carbon steels and cast iron.*

In broken specimens of mild steel, medium steel, hard steel and cast iron, all fractures were always consistent with regular directions. Photographs of fractured specimens of these materials for various values of θ are shown in Fig. 29. Measuring the directions of these fractures, they were found to be in good agreement with the plane of maximum principal stresses. Therefore it was known that fatigue fractures of carbon steels and cast iron are always caused by maximum principal stress, independent of the magnitude of θ.

Whereas, as previously mentioned, the fatigue strength of carbon steels was not consistent with the theory of constant maximum principal stress; that is, mild steel and medium steel are in accordance with the theory of constant shear strain energy as shown in Figs. 18 and 19.

So we may conclude that fatigue fracture and fatigue strength are not decided under the same theory. The reason is due to the fact that in the fatigue tests of these carbon steels, the resistance to the repeated combined stresses of the material comply with the theory of constant shear strain energy and the specimens were subjected to the hardning effect as the fatigue phenomena progressed and became gradually more and more brittle and finally the fractures were caused by the maximum principal stress as in the case of cast iron.

It must be noted that the appearance of fracture, in the specimens of steel failed by torsion at a comparatively high cyclical stress, is not the same as in Fig. 29. Fig. 30 shows the fractures of carbon steels at various values of shear stress ranges. In mild steel, when shear stress range is 15.5 kg/mm^2, there are both longitudinal and inclined fractures, the latter making 45 degrees to the axis of the specimens, and when shear stress range becomes higher, fractures are just perpendicular to the axis of specimens. That is, the fracture of mild steel has the tendency to consist with the direction of maximum shear stress, as the value of shear stress range becomes higher. The same tendency can be seen in medium steel and hard steel. But in medium steel, when shear stress is very high, the specimen fails in many fractures parallel to the longitudinal axis of the specimen. We can suppose these fractures, consistent with the directions of maximum shear stresses, are not caused by true fatigue.

(*2*) *Fra tures of duralumins.*

Fractures of duralumins are quite different from those of steels and cast iron. Specimens failed at various values of θ as shown in Fig. 31. As seen in the figure, fractures of duralumin D-26 are in good agreement with the directions of maximum shear stress. But in duralumin D-24, fractures are not completely similar to those of duralumin D-26; that is, when θ is 0 and 22.5 deg., the fractures are consistent with directions of maximum shear stress, and when θ is 45 and 67.5 deg., the fractures are not the same as duralumin D-26, but make wave form, which is also consistent with the direction of maximum shear stress at the place where direct stress, due to bending, is maximum.* When θ is 90 deg., the fractures were always perpendicular to the axis of specimens. Typical torsional fracture of duralumin at high repeated stress is showh in Fig. 32, which is quite

(*) In the photographs of specimens, the axis of bending moment is always in the plane of paper.

(a) Duralumin D-26.

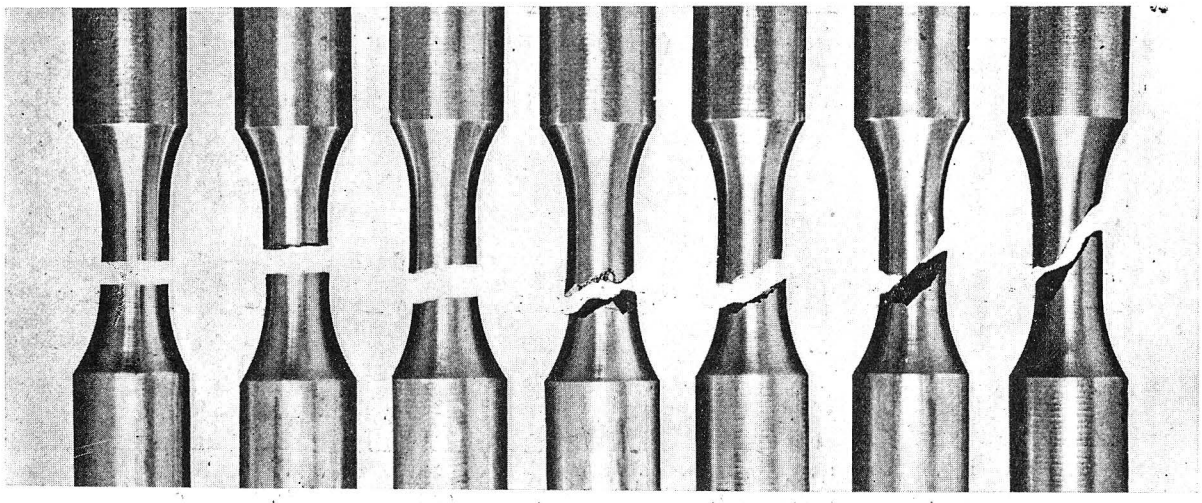

$\theta=0°$ $\theta=15°$ $\theta=30°$ $\theta=45°$ $\theta=60°$ $\theta=75°$ $\theta=90°$

(b) Duralumin D-24.

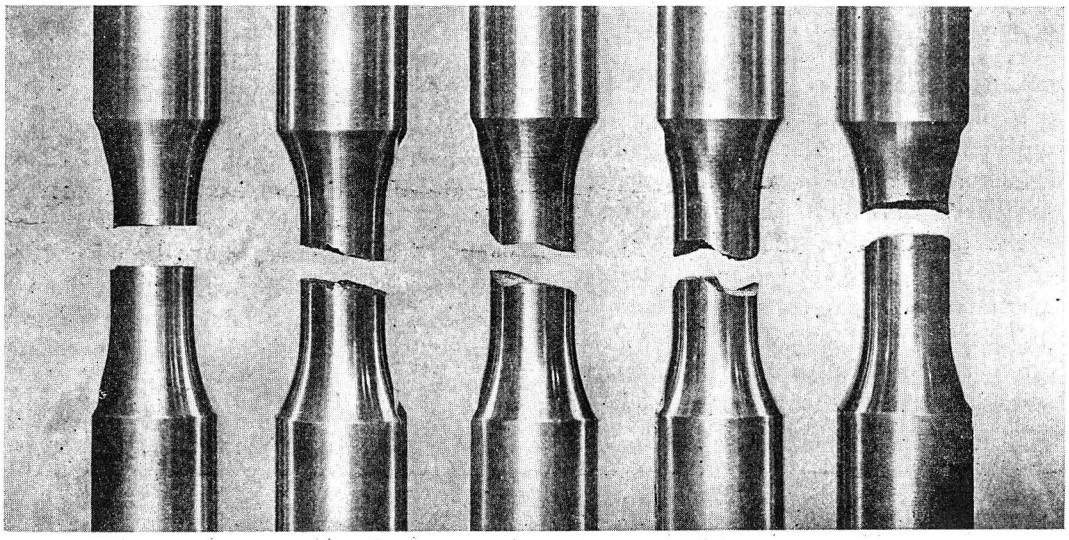

$\theta=0°$ $\theta=22.5°$ $\theta=45°$ $\theta=67.5°$ $\theta=90°$

Fig. 31. Fatigue Fractures of Duralumins.

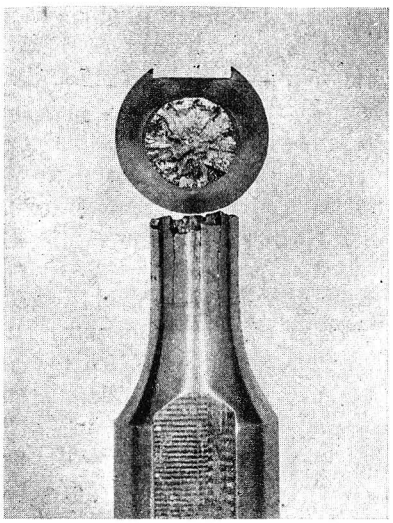

Fig. 32.
Torsional Fracture of Duralmin at High Repeated Stress.

similar to the fracture of medium steel at high torsional stress, as mentioned previously.

Accordingly we can say that fatigue fracture of duralumin is always consistent with the direction of maximum shear stress excluding some specimens in simple bending. But it must be noted that in all specimens shown in Fig. 31, the number of stress cycles to fracture were less than ten million, which is perhaps insufficient for the fatigue test of duralumin. So we cannot confirm from these results whether duralumin fails in the plane of maximum shear stress as in Fig. 31 or not, when the tests are continued to greater stress repetitions.

(3) *Fractures of nickel-chromium steel and brass.*

Fractures of nickel-chromium steel are shown in Fig. 33. As we can see in this figure, fatigue fractures of nickel-chromium steel are consistent neither with the direction of maximum shear stress

(a) Nickel-Chromium Steel, Hot-rolled.

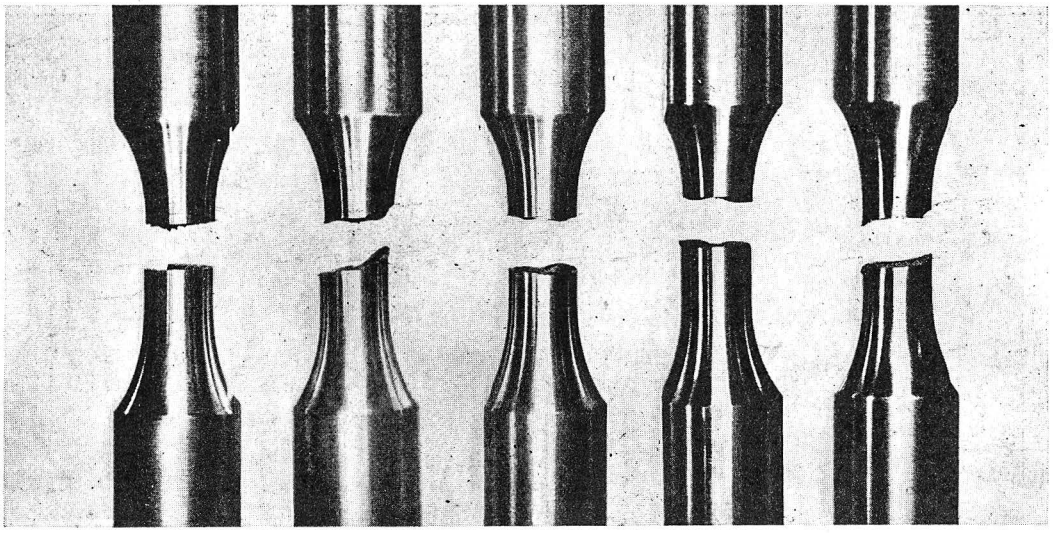

$\theta=0°$ $\theta=22.5°$ $\theta=45°$ $\theta=67.5°$ $\theta=90°$

(b) Nickel-Chromium Steel, Heat-treated.

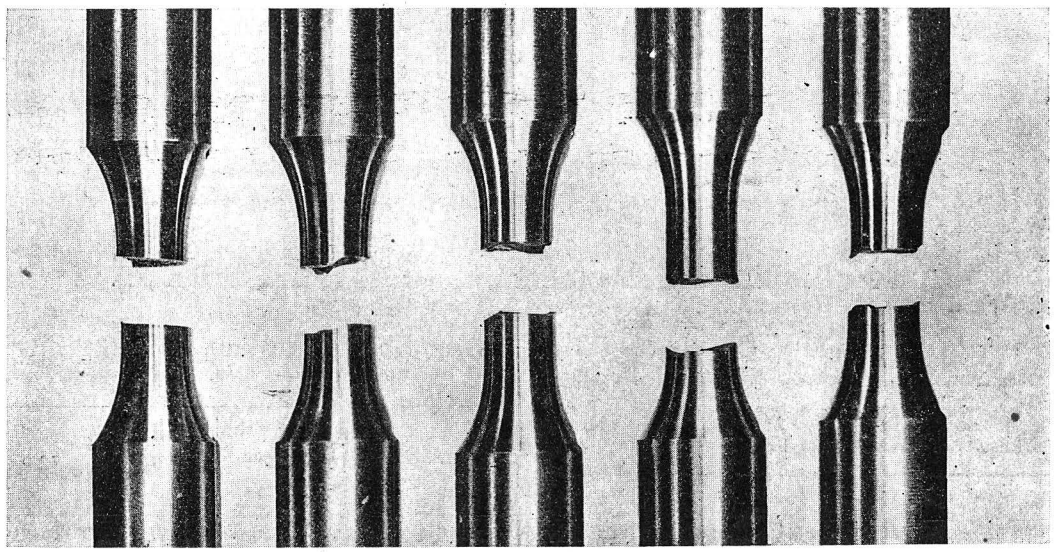

$\theta=0°$ $\theta=22.5°$ $\theta=45°$ $\theta=67.5°$ $\theta=90°$

Fig. 33. Fatigue Fractures of Nickel-Chromium Steel.

nor with principal stress. When θ is 0 or 90 degree, fractures are always perpendicular to the axis of the specimen, and when θ is of other values, fractures make somewhat wave forms.

Fractures of brass are shown in Fig. 34. In this case fractures were very regular, that is, the value of θ is always fairly equal to the angle between the direction of fracture and the axis of the specimen, though in pure torsion, fracture occurs in the directions both parallel and perpendicular to the axis of the specimen.

In nickel-chromium steel and brass, as shown in Fig. 33 and 34, we can hardly establish a reliable theory to explain the mechanism, under which fatigue failures occur. But special attension must be paid to the fact that the fatigue failure due to plane banding is not always similar to that due to rotating bending. Fatigue failures of brass due to rotating bending of cantilever type were in very good agreement with the direction of maximum shear stress as shown in Fig. 35.

VII. Comparison of Fatigue Limits obtained using Rotating Bending Testing Machines and the Combined Stress Testing Machine.

It is of interest to compare the results obtained by the combined stress testing machine with those obtained by the other testing machines. But it has no meaning to compare the values of fatigue limits for torsion, because the combined stress

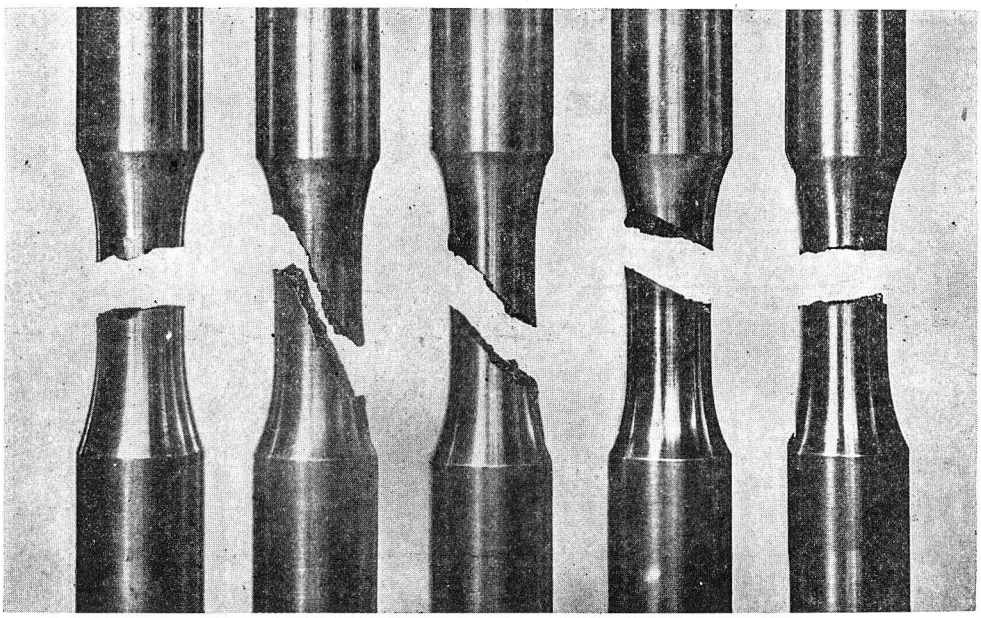

$\theta=0°$ $\theta=22.5°$ $\theta=45°$ $\theta=67.5°$ $\theta=90°$

Fig. 34. Fatigue Fractures of Brass.

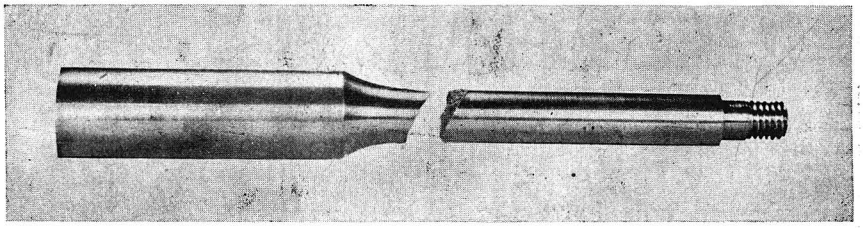

Fig. 35.
Fatigue Fracture of Brass in Rotating Bending Test of Cantilever Type.

Table 13.

Results of Rotating Bending Tests.

Materials	Rotating Bedding Test			Endurance Limit at Plane Bending Test with Combined Stress Testing Machine	$\frac{\sigma'_w}{\sigma''_w}$
	σ kg/mm²	N 10^6	Endurance Limit σ'_w	σ''_w	
Mild Steel	28.0	0.379	25.0	27.0	0.926
	"	0.503			
	26.2	1.659			
	25.0	10.474*			
Medium Steel	25.70	1.979	24.5	24.4	1.004
	23.04	2.662			
	22.80	2.165			
	24.70	3.000			
	24.50	12.560*			
Hard Steel	32	0.171	30	30	1.000
	31	0.487			
	30	10.433*			
Nickel-Chromium Steel, Hot-rolled	44	1.046	40	40	1.000
	42	1.510			
	41	4.488			
	40	10.006*			
Cast Iron	13.0	0.419	11.5	13.0	0.885
	12.0	5.840			
	11.5	10.524*			
Brass	24.6	0.625	12.35	13.4	0.922
	20.0	1.670			
	16.0	7.595			
	13.0	8.964			

* Unbroken specimens.

testing machine and the other ordinary testing machine, such as Nishihara's alternating torsion machine, are essentially of the same type with regard to the impressed conditions of test. While, in regard to bending, it is interesting to compare the results of the combined testing machine with those of rotating bending testing machine, as the stressing conditions in both cases are different.

In making the rotating bending tests, attention is paid to carry on the tests with the same speed and the same diameter of the specimen as in the combined stress tests. Ono's rotating bending testing machine of uniform bending moment type was used for the tests of three

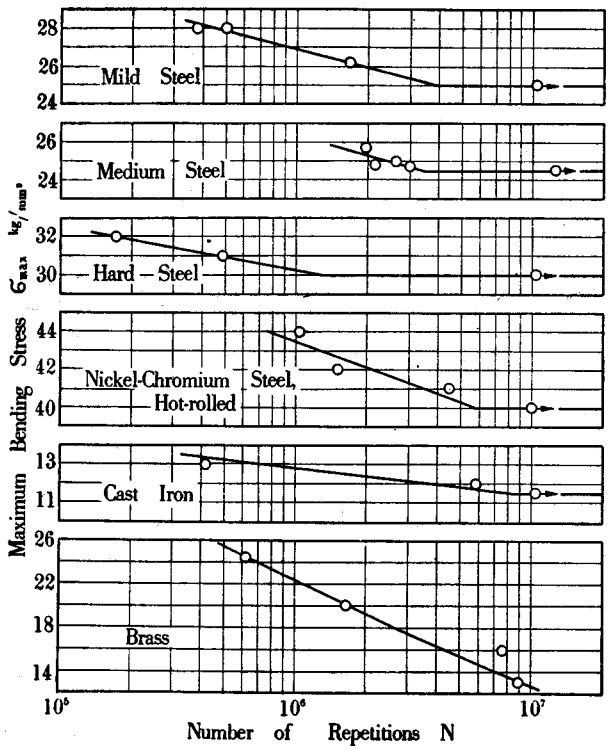

Fig. 36.
Stress-Endurance Cvrves of Rotating Bending Tests.

carbon steels and hot-rolled nickel-chromium steel, while a rotating bending testing machine of the Wöhler type, was used for cast iron and brass, so as to make the diameter of the specimen equal to that of the specimen for combined stress test. For duralumins and heat-treated nickel-chromium steel the rotating bending tests were not made.

Test results are shown in Table 13. Fig. 36 shows the stress-endurance curves. The values of fatigue limits for bending obtained by the combined stress testing machine are added in Table 13. As we can see in the table, the fatigue limits for plane bending are nearly equal to those for rotating bending.

VIII. Conclusions.

(1) A new fatigue testing machine for combined bending and torsion is devised and tests are made for several materials, that is; three carbon steels, an alloy steel, a cast iron, two duralumins and a brass.

(2) Fatigue strength of metalic materials under the combination of bending stress σ and torsional stress τ can be obtained with the following expressions by determining the fatigue limits in pure bending σ_w and pure torsion τ_w experimentally:

$$\sigma^2+\frac{1}{\varphi^2}\tau^2=\sigma_w^2 \qquad \text{for} \quad \varphi=\frac{\tau_w}{\sigma_w}<\frac{1}{\sqrt{3}}$$

$$(1-\varphi^2)\sigma^2+(3\varphi^2-1)\sigma_w\sigma+2\tau^2=2\varphi^2\sigma_w^2$$

$$\text{for} \quad \varphi=\frac{\tau_w}{\sigma_w}>\frac{1}{\sqrt{3}}$$

(3) The value of φ is constant for a given material, independent of the number of stress cycles defined to determine the fatigue strength.

(4) Fatigue fractures of carbon steels are consistent with the plane of maximum principal stresses, though the fatigue resistance is consistent with the theories of constant shear strain energy and constant total energy. This reason lies perhaps in the strain hardning effect due to the repetition of stresses.

Fatigue fractures of duralumins are always consistent with the plane of maximum shear stress excluding some specimens in simple bending.

(5) Fatigue strength for plane bending is equal to or slightly higher than that for rotating bending.

Acknowledgment: The cost of this reserch has been defrayed mostly from the Scientific Research Expenditure of the Ōzi-Seisi Co.